

# Influence of atmospheric deposition on biogeochemical cycles in an oligotrophic ocean system

France Van Wambeke<sup>1</sup>, Vincent Taillandier<sup>2</sup>, Karine Desboeufs<sup>3</sup>, Elvira Pulido-Villena<sup>1</sup>, Julie Dinasquet<sup>4,5</sup>, Anja Engel<sup>6</sup>, Emilio Marañón<sup>7</sup>, Céline Ridame<sup>8</sup>, Cécile Guieu<sup>2</sup>

5

<sup>1</sup> Aix-Marseille Université, CNRS/INSU, Université de Toulon, IRD, Mediterranean Institute of Oceanography (MIO) UM 110, 13288, Marseille, France

<sup>2</sup> CNRS, Sorbonne Université, Laboratoire d'Océanographie de Villefranche (LOV), UMR7093, 06230 Villefranche-sur-Mer, France

10 <sup>3</sup> LISA, UMR CNRS 7583, Université Paris-Est-Créteil, Université de Paris, Institut Pierre Simon Laplace (IPSL), Créteil, France

<sup>4</sup> Sorbonne Universités, Laboratoire d'Océanographie Microbienne (LOMIC), Observatoire Océanologique, 66650, Banyuls/mer, [France](#)

<sup>5</sup> Marine Biology Research Division, Scripps Institution of Oceanography, UCSD, La Jolla, USA

15 <sup>6</sup> GEOMAR – Helmholtz-Centre for Ocean Research, Kiel, Germany

<sup>7</sup> Department of Ecology and Animal Biology, Universidade de Vigo, 36310 Vigo, Spain

<sup>8</sup> Sorbonne University/CNRS/IRD/MNHN, LOCEAN: Laboratoire d'Océanographie et du Climat: Expérimentation et Approches Numériques, UMR 7159, 4 Place Jussieu – 75252 Paris Cedex 05, France

Correspondence to: France Van Wambeke ([france.van-wambeke@mio.osupytheas.fr](mailto:france.van-wambeke@mio.osupytheas.fr)) and  
20 Cécile Guieu ([guieu@jmev-mer.fr](mailto:guieu@jmev-mer.fr))

Supprimé: [obs-vlf](mailto:obs-vlf)

## Abstract.

The surface mixed layer (ML) in the Mediterranean Sea is a well stratified domain characterized by low macro-nutrients and low chlorophyll content, for almost 6 months of the year. In this study we characterize the biogeochemical cycling of N in the ML by analysing simultaneous *in situ* measurements of atmospheric deposition, nutrients, hydrological conditions, primary production, heterotrophic prokaryotic production, N<sub>2</sub> fixation and leucine aminopeptidase activity. Dry deposition was continuously measured across the central and western open Mediterranean Sea and two wet deposition events were sampled, one in the Ionian Sea and one in the Algerian basin. Along the transect, N budgets were computed to compare the sources and sinks of N in the mixed layer. In situ leucine aminopeptidase activity made up 14 to 66 % of the heterotrophic prokaryotic N demand, and the N<sub>2</sub> fixation rate represented 1 to 4.5 % of the phytoplankton N demand. Dry atmospheric deposition of

Supprimé: during

Supprimé: . Nutrient dynamics in the ML depend on allochthonous inputs, through atmospheric deposition and on biological recycling

Supprimé: Here

Supprimé: combining

Supprimé: . The measurements were conducted along a 4300 km transect across the central and western open Mediterranean Sea in spring 2017

Supprimé: on a continuous basis while

Supprimé: . On average, phytoplankton N demand was 2.9 fold higher (range 1.5-8.1) than heterotrophic prokaryotic N demand

Supprimé: contributed

Supprimé: from

inorganic nitrogen, estimated from dry deposition of (nitrate+ammonium) in aerosols, was higher than the N<sub>2</sub> fixation rates in the ML (on average 4.8-fold). The dry atmospheric input of inorganic N represented a highly variable proportion of biological N demand in the ML among the stations, 10 - 82% for heterotrophic prokaryotes and 1-30% for phytoplankton. As some sites were visited for several days the evolution of biogeochemical properties in the ML and within the nutrient-depleted layers could be followed. At the Algerian Basin site, the biogeochemical consequences of a wet dust deposition event was followed with a high frequency sampling of CTD casts. Notably just after the rain, nitrate was higher in the ML than in the nutrient depleted layer below. Estimates of nutrient transfer from the ML to the nutrient depleted layer could explain up to a 1/3 of the nitrate loss from the ML. Phytoplankton did not benefit directly from the atmospheric inputs into the ML, probably due to high competition with heterotrophic prokaryotes, also limited by N and P availability at the time of this study. Primary producers decreased their production after the rain, recovering to their initial state of activity after a 2 day lag in the vicinity of the deep chlorophyll maximum layer.

## 1. Introduction

The Mediterranean Sea (MS) is a semi-enclosed basin characterized by very short ventilation and residence times due to its own thermohaline circulation (Mermex Group, 2011). In terms of biogeochemistry, the MS is characterized by a long summer stratification period. It is a low nutrient, low chlorophyll (LNLC) system with where there is generally an increasing oligotrophic gradient from west to east and an overall deficit in phosphorus (P) compared to nitrogen (N) (Mermex Group, 2011). This is confirmed by an N/P ratio for inorganic nutrients that is higher than the Redfield ratio in deep layers, which increases toward the east (Krom et al., 2004).

The relationship between photoautotrophic unicellular organisms and heterotrophic prokaryotes (competition or commensalism) is affected by the balance of light and nutrients as well as possible inputs of organic matter from river runoff or atmospheric deposition. Phytoplankton generally experience P, N, or NP limitation (Thingstad et al., 2005 ; Tanaka et al., 2011, Richon et al., 2018), whereas heterotrophic prokaryotes are usually P limited, or P and labile carbon co-limited (Sala et al., 2002, Van Wambeke et al., 2002, Céa et al., 2014). The MS receives anthropogenic aerosols continuously, originating from industrial and domestic activities from around the basin and from other parts of Europe along with pulsed natural inputs from the Sahara. It is thus a natural LNLC study area, well adapted to

|   |
|---|
| <b>Supprimé:</b>  |
| <b>Supprimé:</b> Stations   |
| <b>Supprimé:</b> allowed following  |
| <b>Supprimé:</b>  |
| <b>Supprimé:</b> the site in  |
| <b>Supprimé:</b> and on a basis of  |
| <b>Supprimé:</b> before and after a wet dust deposition event,  |
| <b>Supprimé:</b> different scenarios were considered to explain a delayed appearance of peaks in dissolved inorganic phosphate in comparison to nitrate within the ML. After the rain,  |
| <b>Supprimé:</b> fate   |
| <b>Supprimé:</b> out of   |
| <b>Supprimé:</b> Luxury consumption of P by heterotrophic prokaryotes, further transferred in the microbial food web, and remineralized by grazers, is one explanation for the delayed phosphate peak of DIP. The second explanation is a transfer from ML to the nutrient depleted layer below through adsorption/desorption processes on particles. |
| <b>Supprimé:</b> a  |
| <b>Supprimé:</b> , in competition for nutrients with heterotrophic prokaryotes,   |
| <b>Supprimé:</b> s  |
| <b>Supprimé:</b> with respect   |
| <b>Supprimé:</b> a  |
| <b>Supprimé:</b> -  |
| <b>Supprimé:</b> -  |
| <b>Supprimé:</b> gradient of increasing oligotrophy,  |
| <b>Supprimé:</b> deficit  |
| <b>Supprimé:</b> evidenced  |
| <b>Supprimé:</b> higher   |
| <b>Supprimé:</b> ratios   |
| <b>Supprimé:</b> of inorganic nutrients   |
| <b>Supprimé:</b> increasing   |
| <b>Supprimé:</b> 2010   |
| <b>Supprimé:</b> nature of the  |
| <b>Supprimé:</b> experienced by phytoplankton   |
| <b>Supprimé:</b> s  |
| <b>Supprimé:</b> +  |
| <b>Supprimé:</b> continuously   |
| <b>Supprimé:</b> all  |
| <b>Supprimé:</b> and  |
| <b>Supprimé:</b> ,  |
| <b>Supprimé:</b> laboratory   |

135 | investigate the role of ocean–atmosphere exchanges of particles and gases on marine  
biogeochemical cycles. Parameterization and representation of the key processes brought into  
play by atmospheric deposition in the MS must take into account the role of pulsed  
atmospheric inputs (Guieu et al., 2014a). Recent studies describe annual records of  
atmospheric deposition of trace metals and inorganic macronutrients (N, P) obtained at  
several locations around the MS (Markaki et al., 2010; Guieu and Ridame, in press;  
Desboeufs, in press). All records denote the pulsed and highly variable inputs. Recent models  
and observations show that atmospheric deposition of organic matter (OM) is also highly  
variable and that their annual inputs are of the same order of magnitude as river inputs  
(Djaoudi et al., 2017; Kanakidou et al., 2018; Kanakidou et al., 2020; Galetti et al., 2020).  
140 |  
145 | Moreover, the sum of atmospheric inputs of nitrate, ammonium and soluble organic nitrogen  
has been shown to be equivalent or higher than those of N<sub>2</sub> fixation rates (Sandroni et al.,  
2007), although inorganic atmospheric N inputs alone may also be higher than N<sub>2</sub> fixation  
rates (Bonnet et al., 2011).  
150 | Aerosol amendments in bottles, minicosms, or mesocosms have been widely used to study  
trophic transfer and potential export, as they represent to some extent a ‘simplified’ plankton  
trophic web that can be studied along a vertical dimension (i.e. Guieu et al., 2010; Herut et al.,  
2016; Mescioglu et al., 2019). It has been shown that both diversity and functioning of  
various biological compartments are impacted by aerosol additions in different waters tested  
in the MS (Guieu and Ridame, in press, and synthesis Figure 3 therein). Differences in the  
155 | biological responses have been observed, depending on the mode of deposition simulated  
(wet or dry), the type of aerosols used (natural or anthropogenic) and the *in situ*  
biogeochemical conditions at the time of the experiment (Guieu and Ridame, in press).  
Organic carbon from aerosols is partly soluble, and this soluble fraction is partly available to  
marine heterotrophic prokaryotes (Djaoudi et al., 2020). Heterotrophic prokaryotes have the  
160 | metabolic capacity to respond quickly to aerosol deposition through growth and changes in  
community composition (Rahav et al., 2016; Pulido-Villena et al., 2008; 2014), while the  
phytoplankton community responds more slowly or not at all (Guieu and Ridame, in press,  
and reference therein).  
Owing to the intrinsic experimental limitations, which vary depending on the size and design  
165 | of enclosures (i.e. the omission of higher trophic levels, absence of turbulent mixing so  
limiting exchanges by diffusion, and wall effects), such experiments cannot fully simulate *in situ*

**Supprimé:** explore

**Supprimé:** in

**Supprimé:** atmospheric stations located

**Supprimé:** that

**Supprimé:** atmospheric

**Supprimé:** of OM

**Supprimé:** ight

**Supprimé:** ,

**Supprimé:** in the

**Supprimé:** B

**Supprimé:** have been shown to be

**Supprimé:** tested

**Supprimé:** of

**Supprimé:** editerranean

**Supprimé:** ea

**Supprimé:** mimicked

**Supprimé:** used

**Supprimé:** ies

**Supprimé:** slower

**Supprimé:** ,

**Supprimé:** without

**Supprimé:** representation

**Supprimé:** in

**Supprimé:** that

**Supprimé:** ed

**Supprimé:** to

**Supprimé:** ,

195 observations to understand the consequences of aerosol deposition on biogeochemical cycles. Such in situ studies are scarce and require dedicated high frequency sampling to follow the effects of deposition on the biogeochemical processes while taking into account the water column dynamics. To demonstrate this point, the biological response to a Saharan dust event (dust flux = 2.6 g m<sup>-2</sup> recorded at a coastal station in Cap Ferrat) was detected 4 days after the event by only one offshore water column sampling (at the DYFAMED site). An increase in heterotrophic prokaryotic respiration and abundance was observed when compared to a sampling that was carried out 16 days before this dust event (Pulido-Villena et al., 2008). Off the Israeli coast, a moderate natural dust storm (1.05 mg L<sup>-1</sup> over 5 m depth) was followed every 12 hours over 5 days (Rahav et al., 2016). Rapid changes were observed, which could have been missed without high frequency sampling. A decrease in picophytoplankton abundance, an increase in heterotrophic prokaryote abundance, as well as a slight increase in primary production (25%) and heterotrophic prokaryotic production (15%) was observed. Hence, it is necessary to organize sampling surveys with adaptive strategies to follow aerosol deposition events in situ and their impacts on biogeochemical processes, especially in the open waters of the stratified and nutrient limited MS. The objectives of the PEACTIME project were to study fundamental processes and their interactions at the ocean–atmosphere interface following atmospheric deposition (especially of Saharan dust) in the Mediterranean Sea, and how these processes impact the functioning of the pelagic ecosystem (Guieu et al., 2020).

210 215 As atmospheric deposition affects primarily the surface mixed layer (ML), the present study focuses on the upper part of the nutrient depleted layer that extends down to the nutriclines (as defined by Du et al., 2017). During the stratification period, concentrations of nitrate and phosphate inside the ML are often below the quantification limits of standard methods. However, nanomolar concentrations of nitrate (and phosphate) can now be assessed accurately through the Long Waveguide Capillary Cell (LWCC) technique (Zhang and Chi, 2002), which permits the measurement of fine gradients inside nutrient depleted layers of the MS (Djaoudi et al., 2018).

220 225 The aims of the present study were to assess the impact of atmospheric nutrient deposition on biogeochemical processes and fluxes in the open sea during the PEACTIME cruise in the MS. For this we i) estimated nanomolar variations of nitrate concentrations in the surface mixed layer (ML) facing variable inputs of dry and wet aerosol deposition and ii) we compared the aerosol-derived N inputs to the ML with biological activities: primary production,

**Supprimé:** of  
**Supprimé:** the  
**Supprimé:** However,  
**Supprimé:** of aerosol deposition  
**Supprimé:** For instance  
**Supprimé:** of  
**Supprimé:** land  
**Supprimé:** (   
**Supprimé:** )  
**Supprimé:** offshore  
**Supprimé:** observation  
**Supprimé:** , and analysis showed  
**Supprimé:** s  
**Supprimé:** s  
**Supprimé:** by  
**Supprimé:** is on  
**Supprimé:** date  
**Supprimé:** done  
**Supprimé:** In  
**Supprimé:** ,  
**Supprimé:** during  
**Supprimé:** These authors observed rapid  
**Supprimé:** may  
**Supprimé:** They reported a  
**Supprimé:** s  
**Supprimé:** ta  
**Supprimé:** summer  
**Supprimé:** after  
  
**Supprimé:** the  
**Supprimé:** within  
  
**Supprimé:** allows  
**Supprimé:** o  
**Supprimé:** in  
  
**Supprimé:** a  
**Supprimé:** we  
**Supprimé:** s  
**Supprimé:** s

265 heterotrophic prokaryotic production, N<sub>2</sub> fixation and ectoenzymatic activity (leucine  
aminopeptidase). We studied the N budgets along a transect, to include 13 stations crossing  
the Algerian Basin, Tyrrhenian Sea and the Ionian Sea where dry atmospheric deposition was  
continuously measured on board together with seawater biogeochemical, biological and  
270 physical characteristics. We finally focused on a high frequency sampling of a wet deposition  
event that occurred in the western Algerian Basin, where we investigated the evolution of  
biogeochemical fluxes of both N and P and microbial activities.

Supprimé: se  
Supprimé: transect

Supprimé: and

Supprimé: during which

## 2. Materials and Methods

### 2.1 Sampling strategy and measured parameters

275 The PEACETIME cruise (doi.org/10.17600/15000900) was conducted in the Mediterranean  
Sea, from May to June 2017, along a transect extending from the Western Basin to the center  
of the Ionian Sea (Fig. 1). For details on the cruise strategy, see Guieu et al. (2020). Short  
duration stations (< 8 h, 10 stations named ST1 to ST10, Fig. 1) and long duration sites (5  
days, 3 sites named TYR, ION and FAST) were occupied. Chemical composition of aerosols  
280 was quantified by continuous sampling along the whole transect. In addition, two rain events  
were sampled (Desboeufs et al., this issue, in prep), one on the 29<sup>th</sup> of May at ION site, and a  
second one, a dust wet deposition event, at FAST site on the 5<sup>th</sup> of June.

Supprimé: 15

At least 3 CTD casts were conducted at each short station. One cast focused on the epipelagic  
layer (0-250 m), another on the whole water column. Both of these were sampled with a  
285 standard, classical-CTD rosette equipped with a sampling system of 24 Niskin bottles (12 L),  
and a Sea-Bird SBE9 underwater unit equipped with pressure, temperature (SBE3),  
conductivity (SBE4), chlorophyll fluorescence (Chelsea Acquatracka) and oxygen (SBE43)  
sensors. A third cast, from surface to bottom was performed under ‘trace metal clean  
290 conditions’ using a second instrumental package including a titanium rosette (called TMC-  
rosette) mounted on a Kevlar cable and equipped with Go-Flo bottles that were sampled in a  
dedicated clean lab container. The long duration sites were abbreviated as TYR (situated in  
the center of the Tyrrhenian Basin), ION (in the center of the Ionian Basin), FAST (in the  
western Algerian Basin). These 3 sites were selected using satellite imagery, altimetry and  
Lagrangian diagnostics and forecasted rain events (Guieu et al., 2020). At these sites, repeated  
295 casts were performed over a minimum of 4 days, alternating CTD- and TMC- rosettes (Table  
1). The succession of CTD casts at the FAST site is numbered in days relative to a rain event  
collected on board the ship. The first cast of the series was sampled 2.3 days before the rain

Supprimé: Fu  
Supprimé: b  
Supprimé: station

Supprimé: d the second one

Supprimé: The

Supprimé: of

Supprimé: rain

Supprimé: during at least

Supprimé: 5

Supprimé: ,

Supprimé: TYR site was occupied from May 17, 05:08 to May 21, 15:59 and ION site from May 24, 18:02 to May 29, 8:25. FAST site was occupied from June 2, 20:24 to June 7, 23:25 and then from June 8, 21:06 to June 9, 00:16 (all times in local time).

Supprimé: are

Supprimé: that ended on June 5, 3:04

Supprimé: that

event, and the last 2 days after. The FAST site was revisited following the study of ST10 (3.8 days after the rain event). Supprimé: one...2 days after. The FA...

325 Primary production (PP), prokaryotic heterotrophic production (BP), heterotrophic prokaryotic abundances (hprok), ectoenzymatic activities (leucine aminopeptidase (LAP) and alkaline phosphatase (AP)), were determined on water samples collected with the classical CTD-rosette. Dissolved inorganic nutrients, dissolved organic nitrogen (DON) and phosphorus (DOP) were measured on water samples collected using the TMC-rosette. LAP and AP were determined from two layers in the epipelagic waters (5 m depth and deep chlorophyll maximum (DCM)) at the short stations and at the ION and TYR sites. In addition, LAP and AP were determined at 4 depths between 0 and 20 m for 4 profiles at FAST site, to get insight on the variability within the ML. Supprimé: I...organic nutrients, ...

330 Supprimé: Description of the atmospheric deposition strategy is detailed in Desboeufs et al. (this issue, in prep). In summary...or dry deposition estimations ...

335 **2.2 Analytical methods and fluxes calculations**

**2.2.1 Nutrients in the atmosphere**

340 For dry deposition estimations, the total suspended aerosol particles (TSP inlet) were collected continuously throughout the campaign. Aerosol sampling was accomplished by using filtration units on adapted membranes for off-line chemical analysis (Tovar-Sánchez et al., 2020). In parallel to the total aerosol filter sampling, water soluble fractions of the aerosols was sampled continuously, using a Particle-into-Liquid-Sampler (PILS, Orsini et al., 2003). Moreover, two wet deposition events were sampled on board the ship during the cruise, one at the ION site, one at the FAST site using rain collectors with on-line filtration (porosity 0.2 µm) (details in Desboeufs et al., this issue, in prep). Mis en forme Supprimé: by aerosol water extraction unit...sing...a Particle-into-Liquid- ...

345 The nitrate and ammonium concentrations in the aerosols, abbreviated in the text to  $\text{NO}_3$  and  $\text{NH}_4$  respectively, (nitrite concentrations were under analytical detection limits) were analyzed continuously on board from May 13<sup>th</sup>, using PILS sampling coupled on-line with double way ion chromatography (PILS-IC, Metrohm, model 850 Professional IC with Metrosep A Supp 7 column for anion measurements and Metrosep C4 column for cation measurements). The time resolution for PILS-IC analysis was 70 min. for anions and 32 min for cations. Dissolved Inorganic Nitrogen (DIN) fluxes released from the dry deposition were estimated by multiplying the  $\text{NO}_3$  and  $\text{NH}_4$  obtained by PILS-IC measurements, by the dry settling velocities of N-bearing aerosols, i.e. 0.21 and 1 cm s<sup>-1</sup> for  $\text{NH}_4$  and  $\text{NO}_3$ , respectively (Kouvarakis et al., 2001). Mean concentrations were used from the PILS-IC data which were measured (1) during the occupation at each short station lasting between 0.13 and 0.66 days. Supprimé: Nitrate ...itrate and ... Supprimé: by ...ILS sampling couple ... Mis en forme : Exposant Mis en forme Supprimé: Inorganic phosphate (DIP) concentrations were estimated from total phosphorus concentrations in particulate aerosols on filters since it was generally under detection limits using the PILS-IC technique.  $\text{NO}_3$ ,  $\text{NH}_4$  and DIP were also determined by ion chromatography in the dissolved fraction of the 2 rain samples. ... Mis en forme : Couleur de police : Automatique Supprimé: aerosol concentrations of ...

350

355

445 (i.e. enabling on average 5 measurements for NO<sub>3</sub> and 11 measurements for NH<sub>4</sub>), and (2) between two successive casts at the sites with a time lag in between of 0.4 to 1.21 days (i.e. enabling on average 15 measurements for NO<sub>3</sub> and about 30 for NH<sub>4</sub>). At ST1, NH<sub>4</sub> and NO<sub>3</sub> concentrations were obtained using IC analyses following water extraction from aerosol filter sampling as the PILS-IC was not operational.

450 Total dissolved phosphate (TDP) concentrations were estimated from soluble P concentrations extracted from particulate aerosols collected on filters after ultrapure water extraction HR-ICP-MS analysis (Neptune Plus, Thermo Scientific™) (Fu et al., this issue, in prep) since it was generally under detection limits using the PILS-IC technique. The frequency of TDP analysis was therefore less than for DIN: the filters sampled over the duration of the short station (0.28 - 1.15 days depending on the stations). At the 3 sites, filters collected aerosols during periods including each CTD casts sampling date, when possible.

455 Atmospheric deposition flux of soluble P was estimated by multiplying the TDP concentration by a dry settling velocity of 1 cm s<sup>-1</sup>. At the FAST site, a 3 cm s<sup>-1</sup> velocity was used as this value is better adapted for lithogenic particles (Izquierdo et al., 2012).

460 In the rain samples, collected onboard the ship, NO<sub>3</sub>, NH<sub>4</sub> and dissolved inorganic phosphorus (DIP) were also determined using ion chromatography following recovery of the dissolved fraction in the samples. The wet deposition fluxes of these nutrients were then estimated from the measured concentrations in the dissolved fractions from the rain samples, multiplied by total precipitation. Total precipitation was taken from the total hourly precipitation accumulated during the rain event over the region from the ERA5 hourly data reanalysis (Hersbach et al., 2018). Total precipitation was obtained by adding the hourly rainfall onto the grid-points (0.25° x 0.25°) spanning the ship location, more or less 1° around this central grid-point for integrating the regional variability (Table 3). In the rain samples, total particulate P (TPP) and dissolved organic P (DOP) were also available. The dissolved fraction and solution from digestion (Heimburger et al., 2012) of particulate fractions in the filters were analysed by ICP-AES (Inductively Coupled Plasma Atomic Emission Spectrometry, Spectro ARCOS Ametek®) for total particulate TPP. The speciation organic/inorganic of TDP was determined from ICP-MS and IC analysis. DOP was estimated from the difference between TDP, obtained by ICP-MS, and DIP, obtained by ion chromatography.

470

475

## 2.2.2 Nutrients in the water column

|  |
|--|
| <b>Supprimé:</b> averages  |
| <b>Supprimé:</b> during  |
| <b>Supprimé:</b> site  |
| <b>Supprimé:</b> occupations   |
| <b>Supprimé:</b> , except for  |
| <b>Supprimé:</b> where   |
| <b>Supprimé:</b> issued  |
| <b>Supprimé:</b> from filter by  |
| <b>Supprimé:</b> after   |
| <b>Mis en forme :</b> Couleur de police : Automatique  |
| <b>Mis en forme :</b> Couleur de police : Automatique  |
| <b>Mis en forme :</b> Couleur de police : Automatique  |
| <b>Mis en forme :</b> Couleur de police : Automatique  |
| <b>Mis en forme :</b> Couleur de police : Automatique  |
| <b>Mis en forme :</b> Couleur de police : Automatique  |
| <b>Supprimé:</b> This period lasted from 0.13 to 0.66 days for short stations and from 0.41 to 1.21 days for sites.  |
| <b>Supprimé:</b> dry   |
| <b>Supprimé:</b> inorganic P   |
| <b>Supprimé:</b> using   |
| <b>Supprimé:</b> total P particulate   |
| <b>Supprimé:</b> aerosol   |
| <b>Supprimé:</b> multiplied  |
| <b>Supprimé:</b>   |
| <b>Supprimé:</b> except  |
| <b>Supprimé:</b> at FAST site  |
| <b>Supprimé:</b> ,   |
| <b>Supprimé:</b> more  |
| <b>Supprimé:</b> Saharan events  |
| <b>Supprimé:</b> , hence this value is likely an upper range for DIP   |
| <b>Supprimé:</b> At each short station, total P was determined from the filter sampled during the period of the short station and this period of filter collection ranged 0.28 - 1.15 days according to the stations. At the 3 sites, we used filters collecting aerosols during periods including the CTD casts sampling date, when possible. |
| <b>Supprimé:</b> T   |
| <b>Supprimé:</b> filtrate  |
| <b>Supprimé:</b> phase   |
| <b>Supprimé:</b> of  |
| <b>Supprimé:</b> (0.2 µm)  |
| <b>Supprimé:</b> the rain volume and the ...   |
| <b>Supprimé:</b> (Fu et al., this issue, in pre ...)   |

525 Seawater samples for standard nutrient analysis were filtered online ( $< 0.2 \mu\text{m}$ , Sartorius Sartrobran-P-capsule with a  $0.45 \mu\text{m}$  prefilter and a  $0.2 \mu\text{m}$  final filter) directly from the GoFLo bottles (TMC-rosette). Samples collected in acid-washed polyethylene bottles were immediately analyzed on board. Micromolar nitrate + nitrite (NOx) and DIP were determined using a segmented flow analyzer (AAIII HR SealAnalytical©) following Aminot and Kérouel (2007) with a limit of quantification of  $0.050 \mu\text{M}$  for NOx and  $0.020 \mu\text{M}$  for DIP. Samples for the determination of nanomolar concentrations of dissolved nutrients were collected in HDPE bottles previously cleaned with supra-pure HCl. For NOx (considered as NO3 as nitrite fraction was mostly negligible), samples were acidified to pH 1 inside the clean van and analyzed back in the laboratory using a spectrometric method in the visible (540 nm), with a 1 m LWCC (Louis et al., 2015). The limit of detection was 6 nM, the limit of quantification was 9 nM and the reproducibility was 8.5%. DIP was analyzed immediately after sampling using the LWCC method after Pulido-Villena et al. (2010), with a limit of detection of 1 nM (Pulido-Villena et al., 2021). Total dissolved phosphorus (TDP) and nitrogen (TDN) were measured using the segmented flow analyzer technique after high-temperature ( $120^\circ\text{C}$ ) persulfate wet oxidation mineralization (Pujo-Pay and Raimbault, 1994). DOP (DON) was obtained as the difference between TDP (TDN) and DIP (NOx). Labile DOP (L-DOP) was determined as 31% DOP (Pulido-Villena et al., this issue, in prep.).

535

540 Total hydrolysable amino acids (TAAs) were determined as described in detail in Van Wambeke et al. (2021). Briefly 1 ml of sample was hydrolyzed at  $100^\circ\text{C}$  for 20 h with 1 ml of 30% HCl and then neutralized by acid evaporation. Samples were analyzed by high performance liquid chromatography in duplicate according to Dittmar et al. (2009) protocols.

#### 545 2.2.3 Biological stocks and fluxes in the epipelagic waters

Flow cytometry was used for the enumeration of autotrophic prokaryotic and eukaryotic cells, heterotrophic prokaryotes (hprok) and heterotrophic nanoflagellates (HNF). Subsamples (4.5 mL) were fixed with glutaraldehyde grade I 25% (1% final concentration), flash frozen and stored at  $-80^\circ\text{C}$  until analysis. Counts were performed on a FACSCanto II flow cytometer (Becton Dickinson). The separation of different autotrophic populations was based on their scattering and fluorescence signals according to Marie et al. (2000). For the enumeration of hprok (Gasol and Del Giorgio, 2000), cells were stained with SYBR Green I (Invitrogen – Molecular Probes). HNF staining was performed with SYBR Green I as described in

Supprimé: dissolved

Supprimé: to

Supprimé: at

Supprimé: 2020

Supprimé: were

Supprimé: F

Supprimé: by flow cytometry

Supprimé: ,

Supprimé: s

Christaki et al. (2011). All cell abundances were determined from the flow rate, which was calculated with TruCount beads (BD biosciences).

565 Particulate primary production (PP) was determined at 6 layers from the shallow CTD casts Supprimé: on  
(0-250 m) sampled before sun rise. Samples were inoculated with  $^{14}\text{C}$ -bicarbonate and Supprimé: casts  
incubated in on-deck incubators refrigerated using running surface seawater and equipped Supprimé: with  
with various blue screens to simulate different irradiance levels. After 24 h-incubations, Supprimé: during 24 h  
samples were filtered through 0.2 polycarbonate filters and treated for liquid scintillation Supprimé: 2020

570 measurement as described in detail in Marañón et al. (2021). A temperature correction was Supprimé: 2020  
applied as explained in Marañón et al. (2021).  $\text{N}_2$  fixation rates (N2fix) were determined as Supprimé: 2020  
described in Ridame et al. (2011) using 2.3 L of unfiltered seawater (acid-washed Supprimé: this issue, in prep  
polycarbonate bottles) enriched with  $^{15}\text{N}_2$  gas (99 atom%  $^{15}\text{N}$ ) to obtain a final enrichment of Supprimé: Incubations  
about 10 atom% excess. 24 h-incubations for N2fix were conducted under the same Supprimé: Incubations  
temperature and irradiance as the corresponding PP incubations. Supprimé: prokaryotic

575 To calculate heterotrophic prokaryotic production (BP) epipelagic layers (0-250 m) were Supprimé: 2020  
incubated with tritiated leucine using the microcentrifuge technique as detailed in Van Supprimé: occasionally  
Wambeke et al. (2021). We used the empirical conversion factor of 1.5 ng C per pmol of Supprimé: only  
incorporated leucine according to Kirchman (1993). Indeed, isotope dilution was negligible Supprimé: on board  
580 under these saturating concentrations as periodically checked with concentration kinetics. As Supprimé: 2020  
we only used 2 on board temperature controlled dark-incubators, a temperature correction was Supprimé: 2020  
applied as explained in Van Wambeke et al. (2021). Ectoenzymatic activities were measured Supprimé: LAP  
fluorometrically, using the fluorogenic model substrates that were L-leucine-7-amido-4-Supprimé: –  
methyl-coumarin (Leu-MCA) and 4-methylumbelliferyl-phosphate (MUF-P) to track Supprimé: (LAP),  
585 aminopeptidase (LAP), activity and alkaline phosphatase (AP), activity respectively, as Supprimé: (AP),  
described in Van Wambeke et al. (2021). Briefly the release of MCA from Leu-MCA and Supprimé: are  
MUF from MUF-P were followed by measuring the increase of fluorescence in the dark Supprimé: in details  
(exc/em 380/440 nm for MCA and 365/450 nm for MUF, wavelength width 5 nm) in a Supprimé: 2020  
VARIOSCAN LUX microplate reader. Fluorogenic substrates were added at varying Supprimé: V<sub>max</sub>

590 concentrations in 2 ml wells (0.025, 0.05, 0.1, 0.25, 0.5 and 1  $\mu\text{M}$ ) in duplicate. From the Mis en forme : Non Exposant/ Indice  
varying velocities obtained, we determined the parameters  $V_{\text{m}}$  (maximum hydrolysis Supprimé: on  
velocity) and Km (Michaelis-Menten constant that reflects enzyme affinity for the substrate) Supprimé: as well as their corresponding errors by fitting the data using a non-linear regression using the Supprimé: on  
following equation:

$$V = V_m \times S / (K_m + S)$$

where  $V$  is the hydrolysis rate and  $S$  the fluorogenic substrate concentration added. TAA and L-DOP were then used as substrates to determine LAP and AP *in situ* activities using Michaelis-Menten equations (Van Wambeke et al., 2021, Pulido-Villena et al., 2021).

**Supprimé:** ax

**Supprimé:** from

**Supprimé:** 2020

**Supprimé:** this issue, in prep

### 2.3. Vertical partition of the epipelagic layer

The ML can be in a state of stirring and the density and seawater properties are homogeneous, or in a state of rest with homogeneous density but it is the vertical variations in the non-conservative components (such as nutrients); dependent on momentum and heat fluxes at the interface with the atmosphere, that determine the strength and vertical extent of the mixing (Brainerd and Gregg, 1995). In this study, with the absence of concomitant turbulence measurements, the mixed layer depth (MLD) was estimated indirectly using the shape of CTD profiles. Classical methods to evaluate MLD from CTD profiles are based on thresholds of the vertical density gap (de Boyer Montegut et al., 2004; D'Ortenzio et al., 2005) or on the vertical extension of fixed buoyancy content (Moutin and Prieur, 2012).

As discussed in Gardner et al. (1995), the choice of criterion is sensitive to the subtle changes from active mixing to rest, with consequences for the representative time scales of the MLD estimates. In this study, the ML was shallow (10 - 20 m), rapidly activated by the mechanical effects of the wind, and sampled at high frequency (some hours at long duration stations). An approach based on buoyancy criterion has been preferred to resolve short term fluctuations in the mixing state, and MLD was determined as the depth where the residual mass content is equal to  $1 \text{ kg m}^{-2}$ , with an error of estimation of 0.5 m relative to the vertical resolution of the profile (1 m).

In the current case of a shallow ML in such a LNLC system, the nutrient depleted layer comprises the ML and the layer below, referred to hereafter as 'NDLb' (b for bottom or base) when examining the  $\text{NO}_3$  distribution and as PDLb when considering the DIP distributions.

This layer vertically extends between the MLD and the nitracline (phosphacline) depth (Fig.

2). The latter interface is estimated by the depth of the  $\text{NO}_3$  (DIP) depletion density, which is the deepest isopycnal at which micromolar  $\text{NO}_3$  (DIP) is zero (Kamykowski and Zentara, 1985; Omand and Mahadevan, 2015). The  $\text{NO}_3$  (DIP) depletion density is estimated at every discrete profile of micromolar  $\text{NO}_3$  (DIP) concentration by the intercept of the regression line reported in a nutrient-density diagram.

**Supprimé:** 2.3 Enrichment experiments

At the three long duration sites, enrichment experiments were performed using seawater from 5 m depth to assess factors limiting BP in the surface mixed layer. The date of sampling for these experiments [FAST (June 2, 22:00), TYR (May 16, 20:00) and ION (May 25, 20:00)] was before the rain event occurring at FAST and at ION. Eight series of triplicate 60 mL polycarbonate bottles were filled with unfiltered seawater and amended as follows: C : no enrichment, N: +1  $\mu\text{M}$   $\text{NO}_3$  + 1  $\mu\text{M}$   $\text{NH}_4$ ; P: + 0.2  $\mu\text{M}$  DIP; G: + 10  $\mu\text{M}$  C-glucose; NP: N + P; NG : N + G; PG : P + G; NPG: N + P + G. After 48 h incubation in the dark at *in situ* temperature, BP was determined in the 24 bottles (as described in previous section).¶

¶

**Supprimé:** 4

**Supprimé:** of

**Supprimé:** depending

**Supprimé:** e present

**Supprimé:** , in absence of concomitant turbulence measurements

**Supprimé:** a

**Supprimé:** discriminate

**Supprimé:** in

**Supprimé:** e present

**Supprimé:** were

**Supprimé:** better

**Supprimé:** present

**Supprimé:** s

**Supprimé:** a

**Supprimé:** concentration

**Supprimé:** 1986

**Supprimé:** s

There are various mechanisms, dynamical or biological, that can trigger exchanges of nutrients between the ML and NDLb (PDLb). Using the hypothesis of vertical (one-dimensional) regimes, there are two processes of exchange, by diffusion or advection (Du et al., 2017). The flux of nutrient can be expressed as:

$$F_{NO_3} = F_{DIF} + F_{ADV}$$

The diffusive flux  $F_{DIF}$  is expressed by the gradient of nutrient concentration times a vertical diffusivity coefficient  $K_z$  as:

$$F_{DIF} = K_z \times (NO_3_{ML} - NO_3_{NDLb}) / MLD$$

The typical magnitude of  $K_z$  in the surface layers of the PEACETIME stations is assessed to 700 be  $10^{-5} \text{ m}^2 \text{ s}^{-1}$ , as discussed in Taillandier et al. (2020).

The advective flux  $F_{ADV}$  corresponds either to the entrainment of deeper water in the mixed layer due to erosion of the near-surface pycnocline, or to the detrainment of waters below the mixed layer by restratification, depending on the variations in wind stresses and solar heating (Cullen et al., 2002). It is expressed as the variation in the nutrient concentration across the

705 ML times the temporal variation of the MLD, as:

$$F_{ADV} = (NO_3_{ML} - NO_3_{NDLb}) \times dMLD / dt$$

A shallow ML (10 - 20 m) is primarily influenced by wind bursts that lead to intermittent variations of several meters per day ( $10^{-5} \text{ m s}^{-1}$ ) in the MLD. These advective fluxes provide transient exchanges that are one order of magnitude greater than well-established diffusive fluxes. As a consequence, over the time scale of a significant atmospheric deposition, and the associated rapid variations of the MLD, the input of atmospheric nutrients would preferentially be exported below the ML by advection rather than by diffusion. In other terms, using the hypothesis of non-stationary regimes due to rapid changes in atmospheric conditions (that control both the mixing state of the interface and atmospheric nutrient inputs), we 710 assume that vertical advection is the main process of exchange.

At the short stations and sites, the term  $NO_3_{ML} - NO_3_{NDLb}$  can be inferred by the difference between mean nanomolar (LWCC) concentrations inside the NDLb and the mean inside the ML. Since advective flux estimates require knowledge of the evolution of the MLD over time, such fluxes are only accessible at the sites. At short stations, as, advective fluxes could not be characterized, only a qualitative assessment of nutrient fluxes across ML is given. When  $NO_3_{ML} - NO_3_{NDLb} < 0$ , the NDLb is supplied with nutrients across the nutricline, and could be then possibly transferred into the ML. This means that nutrients within the ML are impacted by inputs from below. When  $NO_3_{ML} - NO_3_{NDLb} > 0$ , the ML is supplied in nutrients 715

**Supprimé:** Under

**Supprimé:** are twice

**Supprimé:** e.g.

**Supprimé:** .

**Supprimé:** by

**Supprimé:** of

**Supprimé:** a

**Supprimé:** .

**Supprimé:** With

**Supprimé:** MLD variations

**Supprimé:** some

**Supprimé:** ,

**Supprimé:** t

**Supprimé:** of

**Supprimé:** larg

**Supprimé:** In

**Supprimé:** at

**Supprimé:** rain event

**Supprimé:** atmospheric

**Supprimé:** is

**Supprimé:** under

**Supprimé:** aerosol

**Supprimé:** At

**Supprimé:**

**Supprimé:** stations and long duration

**Supprimé:** sites

**Supprimé:** of

**Supprimé:** inside

**Supprimé:** relative to

**Supprimé:** ones

**Supprimé:** inside

**Supprimé:** the

**Supprimé:** evolution

**Supprimé:** of MLD

**Supprimé:** they

**Supprimé:** long duration sites.

**Supprimé:** and in absence of characterization of

**Supprimé:** can be drawn

**Supprimé:** in

**Supprimé:** inside

**Supprimé:** , meaning

**Supprimé:** ML

from the atmosphere which are further exported into the NDLb. Vertical distributions of DIP, along the longitudinal transect, are described in detail in a companion paper (Pulido-Villena et al., 2021). In this study, we will focus on phosphate exchanges between the ML and PDLb and relationships with NO<sub>3</sub> distribution only at the high-frequency sampled FAST site.

770

Supprimé: above

Supprimé: and

Supprimé: this issue, in prep.).

Supprimé: layers

Supprimé: and relationships with NO<sub>3</sub> distribution

Supprimé: 5

## 2.4 Budget from the metabolic fluxes

Trapezoidal integration was used to integrate BP, PP and N<sub>2</sub>fix within the ML. The biological activity at the surface was considered to be equal to that of the first layer sampled (around 5 m depth at the short stations, 1 m depth at the FAST site). When the MLD was not sampled, the volumetric activity at this depth was linearly interpolated between the 2 closest data points above and below the MLD.

775

We used an approach similar to Hoppe et al. (1993) to compute the *in situ* hydrolysis rates for LAP and AP. We assumed that total amino acids (TAA) could be representative of dissolved 780 proteins. *In situ* hydrolysis rates of LAP and AP were determined using molar concentrations of TAA and L-DOP, respectively and used as the substrate concentration in the Michaelis-Menten kinetics. For LAP, the transformation of *in situ* rates expressed in nmol TAA hydrolyzed L<sup>-1</sup> h<sup>-1</sup> were then transformed into to nitrogen units using N per mole TAA, as the molar distributions of TAA were available. Integrated *in situ* LAP hydrolysis rates were

785

calculated assuming the Michaelis-Menten parameters V<sub>m</sub> and K<sub>m</sub> obtained at a 5 m depth to be representative of the whole ML. Thus an average *in situ* volumetric LAP flux in the ML was obtained by combining the average TAA concentrations in the ML with these kinetic parameters, and multiplying this volumetric rate by the MLD. Daily BP, AP and LAP integrated activities were calculated from hourly rates x 24. Assuming no direct excretion of 790 either nitrogen or phosphorus, the quota C/N and C/P of cell demand is equivalent to the cell biomass quotas. We used molar C/N ratios derived from Moreno and Martiny (2018) (range 6-8, mean 7) for phytoplankton and from Nagata et al. (1986) for heterotrophic prokaryotes (range 6.2-8.4, mean 7.3). C/P of sorted cells (cyanobacteria, picophytoeukaryotes) in P depleted conditions ranged from 107 to 161 (Martiny et al., 2013), and we considered a mean of 130 for phytoplankton. A value of 100 was used for heterotrophic prokaryotes (Godwin and Cotner, 2015).

795

Supprimé: s

Supprimé: , and

Supprimé: t

Supprimé: then

Supprimé: was simply multiplied

Supprimé: ,

Supprimé: 1

## 3. Results

**3.1 Nutrient patterns and biological fluxes along the PEACETIME transect**

815 The ML ranged between 7 m at ST9 and 21 m at ST1 (Table S1, Fig. 3). The nitracline was shallow in the Provençal Basin (50 – 60 m), dropping to 70 m in the Eastern Algerian and Tyrrhenian Seas; becoming deeper in the Western Algerian and Ionian Seas (80 – 90 m, Table S1). Mean NO<sub>3</sub> concentrations in the NDLb ranged from the quantification limit (9 nM) to 116 nM (Table S1, Fig. 4). In the ML, mean NO<sub>3</sub> concentrations ranged from 9 to 135 nM, 820 For the 'group 1' stations (see Table S1), the NO<sub>3</sub> concentrations were low (below 50 nM) within both the ML and the NDLb, with weak differences precluding any gradient between the two layers. For the 'group 2' stations, NO<sub>3</sub> concentrations were moderate (50 - 80 nM) both within the ML and the NDLb but still exhibiting a small difference between the two layers, indicating again no significant instantaneous exchanges. For 'group 3', higher NO<sub>3</sub> concentrations were measured in both the ML and the NDLb (> 80 nM) but the small positive differences (< 20 nM) between the two layers still indicate weak or negligible exchanges between the two layers. For 'group 4', high and moderate NO<sub>3</sub> concentrations were measured within the ML and NDLb, respectively, with a large positive difference (> 20 nM) between the layers. This indicates the presence of a gradient from the ML to the NDLb.

825 At 5 m depth, V<sub>m</sub>LAP ranged from 0.21 to 0.56 nmol MCA-leu hydrolyzed l<sup>-1</sup> h<sup>-1</sup>, and K<sub>m</sub> LAP ranged from 0.12 to 1.29 μM. The mean TAA within the ML ranged from 0.17 to 0.28 μM. From these 3 series of parameters, we derived the mean *in situ* LAP hydrolysis rate within the ML, which ranged from 0.07 to 0.29 nmol N l<sup>-1</sup> h<sup>-1</sup> (results not shown but detailed in Van Wambeke et al., 2021).

830 The vertical distribution of PP and BP for the short stations are described in Marañon et al. (2021). Briefly, PP exhibited a deep maximum close to the DCM depth or slightly above whereas vertical distribution of BP generally showed 2 maxima, one within the mixed layer, and a second close to the DCM. Integrated PP (Table 1, Table S2) ranged from 138 (TYR17 May) to 284 (SD1) mg C m<sup>-2</sup> d<sup>-1</sup>. Integrated BP (0-200 m) ranged from 44 (ION27may) to 840 113 (FAST+0.53) mg C m<sup>-2</sup> d<sup>-1</sup>. Overall, in absence of a rain event the Mediterranean Sea, at the time of the PEACETIME cruise, the transect exhibited the classical west-east gradient of increasing oligotrophy detected by ocean colour (see Fig. 8 in Guieu et al., 2020).

835

**3.2 N budgets and fluxes at short stations**

845 Biological rates (all expressed in N units) within the ML at the short stations were compared (Table 2). Phytoplankton N demand (phytoN demand) was the greatest rate, followed by

**Supprimé:** s...patterns and biological...

**Supprimé:** occupied the first 20 m with an excursion ...anged between 9 ... m in ...

**Supprimé:** NDLb ...O<sub>3</sub> concentration...

**Mis en forme :** Couleur de police : Automatique

**Mis en forme :** Couleur de police : Automatique

**Supprimé:** 5, TYR, 6, 7, ION25 May, FAST+1.05, FAST+2.1 (hereafter 'group 1'). ...he nitrate ...O<sub>3</sub> concentrations we ...

**Mis en forme :** Couleur de police : Automatique

**Supprimé:** Concerning DIP, nanomolar data indicated the presence of positive vertical gradients above the phosphocline, in all stations of the transect, so that DIP in the ML was always lower than in the PDLb above except at ION and ST6 (where no gradient was detected) (Pulido-Villena et al. this issue, in prep.).

**Mis en forme :** Couleur de police : Noir

**Supprimé:** 2020...021) for the short ...

**Mis en forme :** Non Surlignage

**Supprimé:** from 'chlorophyll-rich' waters encountered along the Algerian basin until 'chlorophyll-poor' waters in the Tyrrhenian Sea and 'ultra-poor' surface water in the Ionian Sea.

**Supprimé:** V<sub>m</sub>LAP at 5 m depth ranged from 0.24 to 0.56 nmol MCA-leu hydrolyzed l<sup>-1</sup> h<sup>-1</sup>, and K<sub>m</sub> LAP ranged from 0.12 to 1.29 μM. The mean TAA within the ML ranged 0.17 to 0.28 μM. From these 3 series of parameters, we derived mean *in situ* LAP hydrolysis rate within the ML, which ranged from 0.07 to 0.29 nmol N l<sup>-1</sup> h<sup>-1</sup> (results not shown but detailed in Van Wambeke et al., 2020). ¶

**Supprimé:** Focusing on the surface mixed layer, b...iological rates,...(all ...)

heterotrophic prokaryotic N demand (hprokN demand). On average, phytoN demand was 2.9 times greater than that of hprokN, but with a large variability (min x1.5, max x8.1). LAP hydrolysis rates represented between 14 and 66 % of the hprokN demand (mean  $\pm$  sd : 37%  $\pm$  19%), N<sub>2</sub> fixation rates represented between 1 to 4.5% of the phytoN demand (2.6%  $\pm$  1.3%) and 3 to 11% of the hprok N demand (6.4%  $\pm$  2.4%). N<sub>2</sub> fixation rates integrated over the ML correlated slightly better with hprokN demand ( $r = 0.75$ ) than with phytoN demand ( $r = 0.66$ ). Dissolved inorganic N (DIN=NO<sub>3</sub>+NH<sub>4</sub>) solubilized from dry atmospheric deposition ranged from 17 to 40  $\mu\text{mol N m}^{-2} \text{d}^{-1}$  with on average 79% of this being NO<sub>3</sub> (Table 2). This new DIN input was similar or higher than N<sub>2</sub> fixation rates within the ML (from x1.3 to x11, mean  $\times$  4.8-fold). On average within the ML, the new DIN from dry deposition represented 27% of the hprokN demand (range 10-82%), and 11% of the phytoN demand (range 1-30%).

### 3.3 Biogeochemical evolution at the ION site

The ION site was occupied from the 25<sup>th</sup> to the 29<sup>th</sup> of May. Rain events in the vicinity of the ship were observed on May 26<sup>th</sup> and May 29<sup>th</sup> (Desboeufs et al., this issue, in prep). On the 29<sup>th</sup> of May the rain event was associated with a rain front covering more than 5 000 km<sup>2</sup>. A rain sample could be taken on board between 5:08 and 6:00 (local time), i.e. just 3 hours before the last CTD cast. The chemical composition of the rain indicated an anthropogenic background influence (Desboeufs et al., this issue, in prep.).

TDP solubilized from dry atmospheric deposition decreased from 268  $\text{nmol P m}^{-2} \text{d}^{-1}$  May 25<sup>th</sup>-26<sup>th</sup> to 124  $\text{nmol P m}^{-2} \text{d}^{-1}$  May 27<sup>th</sup>-28<sup>th</sup>. DIN fluxes from dry atmospheric deposition were on average 29  $\pm$  4  $\mu\text{mol N m}^{-2} \text{d}^{-1}$  with no significant difference during the occupation of the site (Table S2). In the rain, the molar ratio DIN/DIP was 208. DOP in the collected rain was also an important source (60%) of the total dissolved P from that wet deposition (Table 3).

CTD casts, dedicated to biogeochemical studies, were taken each 24 h for biological fluxes or 48 h for DIP and NO<sub>3</sub>. Thus the time sequence for nutrients in the water column at ION is given for only by three profiles. The first profile (25<sup>th</sup> of May before rain events in the area) is 'flat', corresponding to fair weather conditions and a shallow ML with low and homogeneous concentrations of NO<sub>3</sub> in the ML and the NDL<sub>b</sub> (Fig. 4). Shortly after, there was an atmospheric depression some events of rain were observed in the area on May 26<sup>th</sup> but not on board, and the ML started to deepen 13 h before the second cast sampling nutrients (on the

Supprimé: *in situ* LAP hydrolysis rates and N<sub>2</sub> fixation... On average, phytoN ...

Supprimé: Dry atmospheric deposition of ...  
Supprimé: was dominated by...ith on ...

Mis en forme  
Supprimé: of inorganic N ...epresents ...  
Mis en forme  
Supprimé: of the phytoN demand

Supprimé: within the ML (range 1-30%).  
Supprimé: long station

Mis en forme : Exposant  
Supprimé: , and the rain event occurred just 3 hours before the last CTD cast. However, rain ... Rain events in the area ...  
Mis en forme : Exposant

Déplacé (insertion) [2]  
Supprimé: DIP...DP solubilized from ...  
Supprimé: and the 28 May down ...o ...  
Mis en forme : Exposant

Supprimé: The percentage of DOP included in rain was also an important P source representing 60% of total dissolved P deposition. ...IN (NO<sub>3</sub>+NH<sub>4</sub>) ...luxes ...

Mis en forme : Exposant  
Déplacé (insertion) [3]  
Supprimé: The rain event collected on board at ION lasted 52 min (Table 3). ...

Supprimé: cast was sampled after the rain, we could not analyze the fate of this wet event in particular its possible effect on biological stocks and fluxes as a function of time. ...  
Mis en forme : Exposant

Supprimé: ...hallow ML with low an...  
Mis en forme : Exposant  
Supprimé: arrived

1120 ~~27<sup>th</sup> of May~~. This cast was marked by high nitrate in the ML (Fig. 3). The mixing should have set up a homogeneous ML, but wind conditions rose to 20 kt just at the time of the cast (Fig. 3). The interval between the second and the third cast sampling nutrients (29<sup>th</sup> of May, cast done 3 hours after the rain sampled on board) is marked by a slight relaxation of weather depression, and a deepening of the ML down to 20 m. This cast was marked by a NO<sub>3</sub> decrease in both the ML and NDLb, but values were higher in ML. Given the remaining signature at 15 m and the deepening of the ML, the two layers might have stayed isolated.

1125 However, the calculation of vertical advective fluxes between the layers showed a downward flux in the first interval 25-27 May (Fig. 4, Table S1) and an upward flux in the second interval (27-29 May).

1130 Due to the lack of high frequency sampling, it was also particularly difficult to assess the direct time evolution effects of dry atmospheric deposition at the ION site. Nevertheless, it was clear from the casts sampled on the 27<sup>th</sup> and 29<sup>th</sup> of May that this site was characteristic of group 4 (i.e. higher NO<sub>3</sub> concentrations in the ML than in the NDLb), indicating recent inputs from the atmosphere. Ectoenzymatic activities were only sampled on the 25<sup>th</sup> of May. Vm of LAP at 5 m (0.22 nmol N l<sup>-1</sup> h<sup>-1</sup>) was one of the lowest values recorded during the cruise whilst Vm of AP showed the highest value (5.6 nmol P l<sup>-1</sup> h<sup>-1</sup>). PP integrated over the euphotic zone increased slightly from 188 to 226 mg C m<sup>-2</sup> d<sup>-1</sup> (Table S2), but due to changes in the MLD at the ION site (range 11-21 m) this trend was not visible when integrating PP over the ML. Integrated over the ML, BP increased slightly, from 7.5 to 10.3 mg C m<sup>-2</sup> d<sup>-1</sup> between the 25<sup>th</sup> and the 29<sup>th</sup> of May, and indicated that hprok benefited more from the atmospheric inputs than the autotrophs as PP decreased at 5m depth (Fig. S1, Table S2). The profiles of hprok and *Synechococcus* abundances showed no particular trend with time, with higher variations within the DCM (Fig. S1).

### 3.4 N budgets and fluxes at the FAST site

1145 During the time at the FAST site, two periods of rains occurred: the evening of June 2nd-3rd and the early morning of the 5th (Tovar-Sanchez et al., 2020). On a spatial scale, the rain radar data indicated the presence of a rain front with patchy, numerous and intense rain events occurring over a large area surrounding the ship's location. These two episodes were concomitant with a dust plume transported in altitude (between 1 and 4 km) and resulted in wet deposition of dust (Desboeufs et al., this issue, in prep.). The second rain event was sampled on board on June 5th (between 02:36 and 03:04, local time) and was associated with

|   |
|---|
| <b>Supprimé:</b> (  |
| <b>Mis en forme :</b> Exposant  |
| <b>Supprimé:</b> )  |
| <b>Supprimé:</b> , which is portioned at 10 m due to the history of the MLD   |
| <b>Supprimé:</b> at   |
| <b>Supprimé:</b> with   |
| <b>Supprimé:</b>  |
| <b>Mis en forme :</b> Exposant  |
| <b>Supprimé:</b> sampled  |
| <b>Supprimé:</b> the  |
| <b>Supprimé:</b> On 29 May,   |
| <b>Supprimé:</b> d  |
| <b>Supprimé:</b> still  |
| <b>Supprimé:</b> ,  |
| <b>Déplacé vers le haut [2]:</b> DIP dry atmospheric deposition decreased from 383 and 385 nmol P m <sup>-2</sup> d <sup>-1</sup> on the 26 and the 28 May down to 185 nmol P m <sup>-2</sup> d <sup>-1</sup> the 30 May. The percentage of DOP included in rain was also an important P source representing 60% of total dissolved P deposition. DIN (NO <sub>3</sub> +NH <sub>4</sub> ) dry atmospheric fluxes could be sampled and daily flux calculated more regularly; it increased from 24 to 34 μmol N m <sup>-2</sup> d <sup>-1</sup> from the 25 to the 28 May and decreased ... |
| <b>Supprimé:</b> DIP dry atmospheric  |
| <b>Déplacé vers le haut [3]:</b> The rain ...   |
| <b>Supprimé:</b> a  |
| <b>Mis en forme :</b> Exposant  |
| <b>Supprimé:</b> The integrated BP increase ...   |
| <b>Supprimé:</b> .¶   |
| <b>Mis en forme :</b> Exposant  |
| <b>Supprimé:</b> mostly   |
| <b>Supprimé:</b> (min-max range of 0.21-0.5 ...   |
| <b>Supprimé:</b> , for a min-max range of 0. ...  |
| <b>Supprimé:</b> 211  |
| <b>Supprimé:</b> (25 May)   |
| <b>Supprimé:</b> 282  |
| <b>Supprimé:</b> 28 May   |
| <b>Supprimé:</b> during the occupation of   |
| <b>Supprimé:</b> Integrated BP (0-200 m) ...  |
| <b>Supprimé:</b> slightly   |
| <b>Mis en forme :</b> Exposant  |
| <b>Supprimé:</b> long station   |
| <b>Supprimé:</b> ¶  |
| <b>Supprimé:</b> occupation of the  |
| <b>Supprimé:</b> site   |
| <b>Supprimé:</b>  |

1250

a dust wet deposition flux  $\sim 40 \text{ mg m}^{-2}$ . The DIN/DIP ratio in the rain reached 480 (Table 3). After the rain, daily fluxes of DIN solubilized from dry aerosol deposition strongly decreased from 45 to  $9.8 \mu\text{mol N m}^{-2} \text{ d}^{-1}$  between June 4th and 5th.

1255

The beginning of the sampling at FAST site (-2.3; -1.5; -0.25) was marked by moderate and similar decreases in NO<sub>3</sub> concentration within the ML and NDLb. Integrated stocks of NO<sub>3</sub> within the ML (Table S2) reflected slight changes with MLD (from 14 to 10 m during this time interval).

1260

On June 5th, the rain event (Table 3) was associated with a strong wind burst and an abrupt mixing. The comparison between NO<sub>3</sub> concentrations from two casts, sampled 6 h before and 6 h after the rain (FAST-0.25 and FAST+0.24), showed a clear N enrichment of the ML as mean NO<sub>3</sub> increased from 56 to 93 nM and NO<sub>3</sub> integrated stocks increased by  $888 \mu\text{mol N m}^{-2}$  (Fig. 3, Table S2). There was also clear difference in the mean NO<sub>3</sub> concentrations between ML and NDLb ( $93 \pm 15$  vs  $51 \pm 7 \text{ nM}$ , respectively). This is the highest NO<sub>3</sub> difference observed during the cruise between these 2 layers (Fig. 4), confirming that this ML enrichment could not be attributed to inputs from below. The relaxation of this wind burst was progressive, with a continuous deepening of the ML (Table S1). The export of the atmospheric NO<sub>3</sub> into the NDLb was maximal after the rain event (FAST+0.24). At the end of the site occupation period (FAST+3.8) high NO<sub>3</sub> concentrations (mean 135 nM) were measured again within the ML.

1265

DIP concentration dynamics were different from NO<sub>3</sub> with the DIP integrated fluxes within the ML similar 6 h before and 6 h after the rain ( $136 \mu\text{mol m}^{-2}$ ). It is only from then on, that DIP flux progressively increased reaching a maximum ( $281 \mu\text{mol P m}^{-2}$ ) one day after the rain (FAST+1).

1270

Immediately after the rain, integrated PP (euphotic zone) decreased from  $274 \text{ mg C m}^{-2} \text{ d}^{-1}$  (FAST-0.9) to  $164 \text{ mg C m}^{-2} \text{ d}^{-1}$  (FAST+0.07) and continued to decrease the following day. It is only 3.8 days after the rain that the initial values (before the rain) of integrated PP could be observed again (Table S2). Such variations were mostly due to changes in volumetric rates within the DCM depth (Fig. S2), as the activity did not change significantly within the ML ( $28\text{--}33 \text{ mg C m}^{-2} \text{ d}^{-1}$ , Fig. S2, Fig. 5). Integrated BP over 0-200 m showed the opposite trend to that of PP and tended to increase after the rain (from  $86 \pm 3 \text{ mg C m}^{-2} \text{ d}^{-1}$  ( $n = 4$ ) before, and up to  $113 \text{ mg C m}^{-2} \text{ d}^{-1}$  (FAST+0.5) after (Table S2)). Although modest, this increasing trend was also visible when integrating BP only over the ML (12-15 before;  $15\text{--}19 \text{ mg C m}^{-2} \text{ d}^{-1}$

1275

**Supprimé:** NO<sub>3</sub> concentration in the ML showed a progressive enrichment with a maximum few hours after the rain event and a smooth decline until the initial conditions were restored 2.3 days after the rain (Fig. 3). Afterwards, the nutrient dynamics was not consistent with this evolution as shown by the high concentrations measured at FAST+3.8. The same analysis can be drawn with respect to exchanges across the ML (Fig. 4, Table S1): NO<sub>3</sub> flux remained low until the rain event, and then a large advective flux is estimated relative to the enrichment of ML and the quick deepening of the ML, this flux declined during the relaxation to initial conditions.¶

Concerning atmospheric wet deposition, the rain event collected on board at FAST lasted 28 min (Table 3). Like for the rain sampled at ION site, DIN flux was much higher than DIP flux, with molar N/P inorganic ratio of 1439, and the percentage of DOP represented 44% of total dissolved P deposition. The chemical composition indicates that the rain sample collected at FAST site was characteristic of a wet dust deposition (Fu et al., this issue, in prep. b) corresponding to a dust deposition of  $12 \text{ mg m}^{-2}$ . This is among the least intense dust deposition fluxes recorded in this area from a long time-series of deposition (Vincent et al., 2016). During FAST site occupation, two periods of rains occurred related to rain fronts (affecting a domain of  $\sim 5000 \text{ km}^2$ ) moving eastward from Spain and North Africa regions: between the evening of June 3 until 5 in the early morning (Desboeufs et al., this issue, in prep.). These two episodes were concomitant with a dust plume transported at altitude (between 1 and 4 km), covering the half of western Mediterranean basin during June 4, and allowed below-cloud deposition of dust (as confirmed by LIDAR records, Desboeufs et al., this issue, in prep.). The rain event collected at FAST site occurred on board after a first night of wet deposition over the whole area and toward the end of the transport of the dust plume. The particulate flux of this collected rain sample was thus likely in the lower range of the wet dust deposition fluxes that had affected the whole area between 3 and 5 June. Indeed, the *in situ* measurements of a dust tracer in the water column (particulate aluminum) show that the total export of particulate matter was rather of the order of  $\sim 55 \text{ mg m}^{-2}$  during the period instead of  $12 \text{ mg m}^{-2}$  as seen in a single collected rain event, and even this value is probably underestimated due to the lack of sampling big dust particles sinking (Bressac et al., this issue, in prep.). After the rain, average daily dry DIN deposition decreased from  $45 \mu\text{mol}$ ...

**Supprimé:** T...e rain event rainfall ... ...

**Supprimé:** However this event can be isolated from the previous sequence and more difficult to interpret as persistence timescales (about 2 days in the hypotheses) are over.¶

**Supprimé:** : ... $274 \text{ mg C m}^{-2} \text{ d}^{-1}$ ... $16$  ...

1565 after). The abundances of picophytoplankton groups were mostly varying in the vicinity of the DCM depth with peaks occurring 1-2 days after the rain (grey profiles, Fig S3), in particular for prokaryotes (*Prochlorococcus*, *Synechococcus*). Heterotrophic prokaryotes and nanoflagellate abundances slightly increased within the DCM depth after the rain.

1570 **4. Discussion**

1575 The specific context of the oceanographic survey constrained the data analysis: biogeochemical responses to a rain event have been scaled in time over a few days (3 - 5), and in space spanning tens of km (40 - 50). Their evolution was restricted to the vertical dimension, integrating lateral exchanges by horizontal diffusion or local advection that occurred over the prescribed space and time scales. In the vertical dimension, exchanges of nutrients across the ML were controlled by advection due to rapidly changing conditions (MLD fluctuations along with nutrient inputs from the atmosphere) rather than to diffusion between stationary pools. Four groups of stations, corresponding to different stages of ML enrichment and relaxation, due to the nutrient inputs from single rain events, have been characterized based on the differences in NO<sub>3</sub> concentration between ML and NDLb (see section 2.4). As shown in Fig. 4, this succession of stages is in agreement with the NO<sub>3</sub> fluxes from above and below the ML. Moreover, they provide a temporal scaling of the oceanic response to atmospheric deposition, with a quasi-instantaneous change at the time of the rain event and a 2-day relaxation period to recover to pre-event conditions

1585 In this context, we will i) discuss the nitrogen budget within the ML at the short stations considered as a 'snapshot', and ii) analyze in detail, using a time series of CTD casts, the biogeochemical changes within the ML and the NDLb following the atmospheric wet deposition event at the FAST site, discussing the possible modes of transfer of nutrients between these 2 layers.

1590 **4.1 A snapshot of biological fluxes in the ML and their link to new DIN from atmospheric dry deposition**

1595 The dependence of hprok on nutrients rather than on labile organic carbon during stratification conditions is not uncommon in the MS, (Van Wambeke et al., 2002, Céa et al., 2017; Sala et al., 2002) and has also been shown during PEACETIME cruise (P, or N,P colimitation, Fig. S4). Hprok have an advantage due to their small cell size, and their kinetic

**Supprimé:** around

**Supprimé:** also

**Supprimé:** ¶

**3.5 Enrichment experiments at long stations¶**

At TYR site, BP was significantly stimulated only after addition of 2 major elements, with a greater response with PN and NPG combinations (Fig. 6). At ION site, BP was primarily limited by P availability, as only combinations with P, single or in combination with other elements, stimulated BP whereas all other combinations of enrichment did not stimulate BP significantly compared to the control. At FAST site, BP was primarily limited by N availability, as all combinations with N, single or in combination with other elements, stimulated BP. However at this site it is likely that BP was also co-limited by 2 elements, as G addition alone also stimulated BP. Note that the PN combination has induced a higher stimulation of BP than other double combinations (NG or PG).¶

**Supprimé:** In this study, *in-situ* characterization of the biogeochemical response to atmospheric deposition was studied for the surface mixed layer (ML) at the interface with the atmosphere.

**Supprimé:** at

**Supprimé:** and

**Déplacé (insertion) [4]**

**Supprimé:** different

**Supprimé:** using the qualitative ...

**Supprimé:** .

**Supprimé:** s

**Supprimé:** discuss the classification of ...

**Supprimé:** i

**Supprimé:** finely

**Supprimé:**

**Supprimé:** site along with

**Supprimé:** ¶

**Déplacé vers le haut [4]:** Four ...

**Mis en forme :** Non Surlignage

**Mis en forme :** Non Surlignage

**Supprimé:** 2

**Supprimé:** dry

**Supprimé:** Enrichment experiments ...

**Supprimé:** sources suggests that they ...

**Supprimé:** . This is consistent with oth ...

**Supprimé:** Under such conditions of ...

**Supprimé:** of

**Supprimé:** -

**Supprimé:** d cells

systems which are adapted to low concentration ranges of nutrients (for example for DIP see Talarmin et al., 2015). Under such conditions of limitation, hprok will react rapidly to new phosphorus and nitrogen inputs, coming from atmospheric deposition. During an artificial *in situ* DIP enrichment experiment in the Eastern Mediterranean, P rapidly circulated through hprok and heterotrophic ciliates, while the phytoplankton was not directly linked to this 'bypass' process (Thingstad et al., 2005). Bioassays conducted in the tropical Atlantic Ocean have also shown that hprok respond more strongly than phytoplankton to nutrients from Saharan aerosols (Marañón et al. 2010), a pattern that has been confirmed in a meta-analysis of *in vitro* dust addition experiments (Guieu and Ridame, in press; Gazeau et al., 2021).

Supprimé: , that

Supprimé: like

Supprimé: those

Supprimé: coming

Supprimé: the

Supprimé: e

Supprimé: et al. 2014a

We considered hprokN demand together with phytoN demand and compared it to autochthonous (DON breakdown by ectoenzymatic activity) and allochthonous (atmospheric deposition) sources. To the best of our knowledge this is the first time that these fluxes are compared based on their simultaneous measurements at sea. A high variability was observed between the 10 short stations (Table 2). The regeneration of nitrogen through aminopeptidase activity was clearly the primary provider of N to hprok as 14 to 66% (mean ± sd : 37% ± 19%) of the hprokN demand could be satisfied by *in situ* LAP activity. Such percentages may be largely biased by the conversion factors from C to N and propagation of errors for the LAP hydrolysis rates and BP rates. However, the C/N ratio of hprok is relatively narrow under large variations of P or N limitation (6.2 to 8.4; Nagata, 1986). Other regeneration sources exist such as direct excretion of NH4 or low molecular weight DON sources with no necessity for hydrolysis prior to uptake (Jumars et al., 1989). For instance, Feliú et al. (2020) calculated that NH4 and DIP excretion by zooplankton would satisfy 25-43% of the phytoN demand and 22-37% of the phytoP demand over the whole euphotic zone. Such percentages suggest that direct excretion by zooplankton along with ectoenzymatic activity, provide substantial N for biological activity.

N<sub>2</sub> fixation is also a source of new N that can directly fuel hprok as some diazotrophs are heterotrophic (Delmont et al. 2018, and references therein), or indirectly, as part of the fixed N<sub>2</sub> that rapidly cycles through hprok (Caffin et al., 2018). Furthermore, it has been observed that there is a better coupling of N<sub>2</sub>fix rates with BP rather than with PP in the eastern MS (Rahav et al., 2013b). This was also observed within the ML in this study. Our data sho that the hypothetical contribution of N<sub>2</sub>fix rates to hprokN demand within the ML was low, (6.4 ± 2.4%) and consistent with the low N<sub>2</sub>fix rates observed in the MS (i.e. Rahav et al., 2013a;

Supprimé: (atmospheric deposition).

Supprimé: are

Supprimé: on board

Supprimé: among

Supprimé: first

Supprimé: :

Supprimé:

Supprimé: like

Supprimé: of

Supprimé: and 22-37%

Supprimé: of the whole euphotic zone

Supprimé: , respectively

Supprimé: in addition to

Supprimé: also substantially

Supprimé: s

Supprimé: also

Supprimé: directly

Supprimé: diazotrophs

Mis en forme : Non Exposant/ Indice

Supprimé: has been observed

Supprimé: 2013a

Supprimé: For this reason, we also examined a

Supprimé: : it

Supprimé: ,

Supprimé: ranging from

Supprimé:

Supprimé: 1 to 4.5 %

Supprimé: . It is

Supprimé: .

Supprimé: 2013b

1865 Ibello et al., 2010; Ridame et al., 2011; Bonnet et al., 2011). This differs from other parts of the ocean, primarily limited by N but not P, such as the south eastern Pacific where N<sub>2</sub> fixation rates are high (Bonnet et al., 2017) and can represent up to 81 % of the hprokN demand (Van Wambeke et al., 2018).

1870 Considering LAP as the most relevant regeneration source of N, it is clear that even the sum of LAP activity and N<sub>2</sub> fixation were not sufficient to meet hprokN demand (cumulated, these fluxes contributed 19 to 73% of HbactN demand). The last source of new N we examined was DIN released by dry atmospheric deposition. Such DIN fluxes presented a low variability along the transect (29 ± 7 µmol N m<sup>-2</sup> d<sup>-1</sup> at the short stations) and were among the lowest measured in the Mediterranean environment, which normally ranges from 38 to 240 µmol N m<sup>-2</sup> d<sup>-1</sup> (Desboeufs et al., in press). It has to be noted that the fluxes measured during the PEACETIME cruise are representative of the open sea atmosphere while published fluxes were measured at coastal sites where local/regional contamination contributes significantly to the flux (Desboeufs, in press). Atmospheric deposition also delivers organic matter (Djaoudi et al., 2017, Kanakidou et al., 2018), which is bioavailable for marine hprok (Djaoudi et al., 2020). Dissolved organic nitrogen (DON) released from aerosols, not determined here, can be estimated from previous studies. DON solubilized from aerosols contributes 19 to 42% of the total dissolved N released from dry deposition in the MS (Desboeufs, in press), with an average of 32%. Considering this mean, DON released from dry deposition was estimated to range from 8 to 19 µmol N m<sup>-2</sup> d<sup>-1</sup> at the short duration stations. The total dissolved N solubilized from dry deposition (inorganic measured + organic estimated) would thus represent 14 to 121% of the hprokN demand. Because of the low variability in DIN (and estimated DON) fluxes derived from dry deposition, the atmospheric contribution was mainly driven by biogeochemical conditions and not by the variability of atmospheric fluxes during the cruise (CV of Nprok N demand and phyto N demand at the short stations were 45% and 89%, respectively, and that of DIN flux 25%). However, the calculated contribution can also be biased by the deposition velocity used to calculate DIN solubilized from the dry deposition. Deposition velocity was set at 1 cm sec<sup>-1</sup> for NO<sub>3</sub> and 0.21 cm sec<sup>-1</sup> for NH<sub>4</sub>. As NO<sub>3</sub> was the dominant inorganic form released by dry deposition, it is clear that the choice of 1 cm sec<sup>-1</sup> for NO<sub>3</sub> influenced its contribution. This choice was conditioned by the predominance of NO<sub>3</sub> in the large mode of Mediterranean aerosols such as dust or sea salt particles (e.g., Bardouki et al., 2003). However, the deposition velocity of NO<sub>3</sub> between fine and large particles could range from 0.6 to 2 cm sec<sup>-1</sup> in the Mediterranean aerosols (e.g.

|   |
|---|
| <b>Supprimé:</b> , in comparison to   |
| <b>Supprimé:</b> s  |
| <b>Mis en forme :</b> Indice  |
| <b>Supprimé:</b> 3 to   |
| <b>Supprimé:</b> N  |
| <b>Supprimé:</b> those  |
| <b>Supprimé:</b> With hprok primarily limited by the availability of N, P or colimited NP, we thus examined possible N sources provided by the atmosphere (P sources at the short stations are discussed in Pulido-Villena et al., this issue, in prep.). |
| <b>Supprimé:</b> D  |
| <b>Supprimé:</b> DIN  |
| <b>Supprimé:</b> fluxes   |
| <b>Supprimé:</b> recorded   |
| <b>Supprimé:</b> for  |
| <b>Supprimé:</b> but were obtained offshore compared to other   |
| <b>Supprimé:</b> measurements   |
| <b>Supprimé:</b> carried out  |
| <b>Supprimé:</b> On a yearly survey, based on 10 aerosols collectors all around coastal sites of the Mediterranean Sea, dry DIN deposition was very patchy in space and time with an average of 38 µmol N m <sup>-2</sup> d <sup>-1</sup> ...             |
| <b>Supprimé:</b> fluxes   |
| <b>Supprimé:</b> include  |
| <b>Supprimé:</b> Soluble  |
| <b>Supprimé:</b> was unfortunately  |
| <b>Supprimé:</b>  |
| <b>Supprimé:</b> total N dry deposition in  |
| <b>Supprimé:</b> ; Galletti et al., 2020  |
| <b>Supprimé:</b> a  |
| <b>Supprimé:</b> of 32%,  |
| <b>Supprimé:</b> d  |
| <b>Supprimé:</b> sampling   |
| <b>Supprimé:</b> flux provided  |
| <b>Supprimé:</b> by   |
| <b>Supprimé:</b> the  |
| <b>Supprimé:</b> atmospheric  |
| <b>Supprimé:</b> from   |
| <b>Supprimé:</b> Such concomitant   |
| <b>Supprimé:</b> percentages  |
| <b>Supprimé:</b> assumptions on the   |
| <b>Supprimé:</b> We considered averages d   |
| <b>Supprimé:</b> ting   |
| <b>Supprimé:</b> largely  |
| <b>Supprimé:</b> is   |

1955 Sandroni et al., 2007). Even considering the lower value of  $0.6 \text{ cm sec}^{-1}$  from the literature, the contribution of DIN from atmospheric dry deposition to hprokN demand within the ML would still be significant (up to 72%).

#### 4.2 Biogeochemical response after a wet event – N and P budgets at FAST site

1960 Rain events are more erratic than dry atmospheric deposition but represent on average much higher new nutrient fluxes to the MS surface waters on an annual basis, e.g. 84% of annual atmospheric DIN fluxes in Corsica Island (Desboeufs et al., 2018). On the scale of the Mediterranean basin, the annual wet deposition of DIN was found to be 2-8 times higher than DIN from dry deposition (Markaki et al., 2010). Wet deposition also contributes significantly to DON atmospheric fluxes in the MS: For example at Frioul Island (Bay of Marseille, NW MS), total (wet + dry) DON atmospheric fluxes ranged between 7 and  $367 \mu\text{mol DON m}^{-2} \text{ day}^{-1}$  and represented  $41 \pm 14\%$  of the total atmospheric nitrogen flux (Djaoudi et al., 2018). In the Eastern MS (Lampedusa Island) DON atmospheric fluxes ranged between 1.5 and  $250 \mu\text{mol DON m}^{-2} \text{ day}^{-1}$  contributing to 25% of the total atmospheric nitrogen flux, respectively (Galletti et al., 2020). In both studies, bulk atmospheric fluxes of DON were positively correlated with precipitation rates, indicating the preponderance of wet deposition over dry deposition.

1975 At the FAST site, the maximum net variations of NO<sub>3</sub> and DIP concentrations within the ML before/after the rainy period reached  $1520-665 = \pm 855 \mu\text{mol N m}^{-2}$  for NO<sub>3</sub> and  $281-137 = \pm 144 \mu\text{mol P m}^{-2}$  for DIP (Table S2). In other terms, based on a mean MLD of 16 m, the net observed increases in the ML were + 9 nM DIP and + 54 nM NO<sub>3</sub>. As the rain event in the area would have increase by 0.07 nM DIP and 21 nM NO<sub>3</sub> concentrations over the whole mixed layer, the net variations observed in the ML are thus higher than the calculated variation in stocks deduced from the N and P concentrations of this rain event (Table 3). This is still true when including all P or N chemical forms (particulate and soluble, inorganic + organic fractions). For example the P concentration in the ML would increase by ~0.68 nM. As described in the results section 3.4, the rains affecting the FAST site were spatially patchy over a large area (~40-50 km radius around the R/V). Thus, we could consider that the biogeochemical impacts observed at FAST site were probably due to a suite of atmospheric events rather than due to the single event collected on board. It is possible that meso- and sub-

**Supprimé:** , and

**Supprimé:** We examined if the four groups of stations described in results section 3.1 and based on NO<sub>3</sub> distribution were also characterized by particular biological fluxes. Although a large variability of biological activities were observed in the ML among those 4 groups, some trends were depicted. LAP activity in ML was higher at the stations of group 1 (with lowest NO<sub>3</sub> concentration in ML and NDLb), in comparison to the group 4 (which exhibited the larger difference of concentrations between ML and NDLb) ( $121 \pm 54$  compared to  $46 \pm 23 \mu\text{mol N L}^{-1} \text{ d}^{-1}$ , respectively). The stations from group 1 also presented the lowest DIN dry deposition flux ( $26 \pm 6 \mu\text{mol N m}^{-2} \text{ d}^{-1}$ ). Finally, it was always in a station from group 4 that the higher phytoN demand, HbactN demand and N2fix rates were detected. Part of the variability obtained among the different groups was also related to the instantaneous character of comparison. Indeed, it is clear that a succession of biogeochemical changes occurs at different time scales during an atmospheric deposition event. Such comparison as a function of time was ...

**Supprimé:** provide

**Supprimé:** yearly...nnual atmospheric ...

**Supprimé:** that of

**Supprimé:** also ...significantly to DON ...

**Supprimé:** <sup>1</sup> in the NW MS (Frioul Island; Djaoudi et al., 2018)

**Supprimé:** ...41 ± 14% of the total ...

**Supprimé:** and...between 1.5 and 250 ...

**Supprimé:** The coupled atmospheric and biogeochemical water column sampling ...

**Mis en forme :** Surlignage

**Supprimé:** long duration ...AST static ...

**Supprimé:** The

**Supprimé:** accumulation ...ariations q ...

**Supprimé:** ,

**Supprimé:** (data from FAST+1.05 relative to FAST-0.25)

**Supprimé:** variations

**Supprimé:** collected on board...vent if ...

**Supprimé:** r...ncrease byeleased ...

**Supprimé:** 008 ...7 nM DIP and 7 ...

**Supprimé:** .

**Supprimé:** in particular

**Supprimé:** particu

**Supprimé:** DI... (Table 4). ...his is st ...

**Supprimé:** the total atmospheric deposition

**Supprimé:** this ...ould increase by ...

mesoscale dynamics encountered at FAST site (Figs 5 and 12 in Guieu et al., 2020) can explain such cumulative impact.

Interestingly, a delay of about 19 h was observed in the maximum net accumulation within the ML between DIP (FAST+1.05) and NO<sub>3</sub> (FAST+0.24). The DIN/DIP ratio in the rain (1438) was much higher than the Redfield ratio. As the biological turnover of DIP in the MS is rapid (from min to few h, Talarmin et al., 2015), new DIP from rain might have behaved differently than DIN. Two different mechanisms can explain this delay: (i) processes linked to bypasses and luxury DIP uptake (storage of surplus P in hprok before a rapid development of grazers (Flaten et al., 2005; Herut et al. 2005, Thingstad et al., 2005) that are later responsible for DIP regeneration so that DIP net accumulation is delayed and/or (ii) abiotic processes such as rapid desorption from large sinking particles followed by adsorption of DIP onto submicronic iron oxides still in suspension as observed experimentally in Louis et al. (2015).

The first proposed mechanism may be supported by the observed increase of BP, along with a stable PP which suggests an immediate benefit of the new nutrients from rain by hprok rather than phytoplankton. The so-called luxury DIP uptake by the competing organisms like hprok is efficient (small cells with high surface/volume ratio and DIP kinetic uptake adapted to low concentrations). It is of course difficult to quantify such *in situ* variations in comparison to mesocosms/minicosms dust addition experiments, in which clearly heterotrophy is favoured first (Marañón et al., 2010; Guieu et al., 2014b; Gazeau et al., 2021). Few attempts in the field have confirmed these trends (Herut et al., 2005, Pulido-Villena et al., 2008) but, as stated in the introduction, these studies lacked high frequency sampling.

The second proposed mechanism, the abiotic desorption/adsorption, is compatible with the observed 19 h delay (Louis et al., 2015). Note that most of the estimates of such abiotic processes are from dust addition experiments with contrasting results, some showing this abiotic process of absorption/desorption while the particles are sinking (Louis et al., 2015), and other not (Carbo et al., 2005) or showing it as negligible in batch experiments (Ridame et al., 2003). It is possible that DIP adsorbed onto large particles rapidly sinks out of the ML, and desorbs partly during its transit in the PDLb, where it could stay longer thanks to the pycnoclines barriers.

We tentatively made a P budget between FAST+1.05 and FAST+2.11 where a net decrease of DIP (-87  $\mu\text{mol P m}^{-2}$ ) was observed in the ML. During this time, advective flux of DIP toward the PDLb was not detectable as DIP concentrations within the ML were always lower than within the PDLb (Pulido-Villena et al., 2021.). This indicated that the DIP was assimilated

Supprimé:

Supprimé:

Supprimé:

Supprimé: One reason for this discrepancy might be, as developed in section 3.4, that the collected rain sampled on board represented only a fraction of the whole rain episode that affected a large area around the ship. Based on aluminum inventory in the water column (Bressac et al., this issue, in prep.), the total dust deposition having affected the FAST site was 4.6 times higher on the same order ( $55 \text{ mg m}^{-2}$ ) than the dust flux measured deducted from our single rain event ( $12.40 \text{ mg m}^{-2}$ ). It is likely that the deduced new N and P increases within the ML due to the collected rain are well still underestimated. If we consider the above cited factor of  $4.655 \text{ mg m}^{-2}$ , the atmospheric flux could have provided an addition of about  $33.29 \text{ nM}$  for NO<sub>3</sub> and  $0.037.09 \text{ nM}$  for DIP ( $0.35.94 \text{ nM}$  total P) in the ML, more in agreement with the marine volumetric variation, at least for NO<sub>3</sub>, and suggesting even that atmospheric nitrate input could alone explain the increase of NO<sub>3</sub> in the ML.

Supprimé: A

Supprimé: Mediterranean Sea

Supprimé: this indicates that

Supprimé: provided by

Supprimé: be proposed to

Supprimé: the observed

Supprimé: on,

Supprimé: a

Supprimé: process

Supprimé: evidenced

Supprimé: is efficient

Supprimé: *in situ*

Supprimé: 2020

Supprimé: have been already described,

Supprimé: confirming

Supprimé: described

Supprimé: o

Supprimé: however

Supprimé: Analysis of abiotic processes have been tentatively done through lab ...

Supprimé: their

Supprimé: they

Supprimé: :

Supprimé: at

Supprimé: was

Supprimé: this issue, in prep

Supprimé: this

and/or transformed to DOP via biological processes, and/or adsorbed onto particles and then  
2280 exported to PDLb by sedimentation. By integration of PP and BP over this period (34.5 and  
19.7 mg C m<sup>-2</sup>, respectively) and, by assuming that all the disappearing 87 µmol DIP m<sup>-2</sup>  
would be consumed by hprok and phytoplankton, we could estimate a C/P ratio reached in  
their biomass of ((34.5+19.7)/12~~x~~1000)/87=52. Such C/P suggests that DIP was not limiting  
these organisms anymore. Indeed a decrease of C/P quotas may highlight a switch from P to  
2285 C limitation for heterotrophic bacteria (Godwin and Cotner, 2015) and from P to N limitation  
or increased growth rates for phytoplankton (Moreno and Martiny, 2018). Furthermore, as  
DIP is also recycled via alkaline phosphatase within the ML, we also consider another source  
of DIP via alkaline phosphatase activity, from which *in situ* activity (see Van Wambeke et al.,  
2290 2021 for *in situ* estimates) could release 139 µmol DIP m<sup>-2</sup> during this period. Assuming also  
that DIP resulting from of AP hydrolysis was fully assimilated for P biological needs, then  
C/P ratio would be (((34.5+19.7)/12~~x~~1000))/(87+139) =19. This low ratio seems unrealistic  
for phytoplankton (Moreno and Martiny, 2018) as well as hprok, even growing in surplus C  
conditions (Makino et al., 2003; Lovdal et al., 2008; Godwin and Cotner, 2015).  
Some of the P recycled or brought into the ML from atmospheric deposition has consequently  
2295 been exported below the ML. DIP is abiotically adsorbed on mineral dust particles (Louis et  
al., 2015), most of them sinking, and thus constitute a source of export out of the ML. It is  
also possible that such sorbing process on dust particles enables the export of other P-  
containing organic molecules, for instance DOP or viruses produced following luxury DIP  
assimilation. Free viruses, richer in P than N relative to Hprok, could adsorb, like DOM, onto  
2300 dust particles and constitute a P export source. Indeed, free viruses sorb onto black carbon  
particles, possibly reducing viral infection (Mari et al., 2019; Malits et al., 2015). However,  
particle quality is a determining factor for DOM or microbial attachment, and what has been  
shown for black carbon particles is not necessarily true for dust particles. For instance the  
addition of Saharan dust to marine coastal waters led to a negligible sorption of viruses to  
2305 particles and increased abundance of free viruses (Pulido-Villena et al., 2014), possibly linked  
to an enhancement of lytic cycles in the ML after relieving limitation (Pradeep Ram and  
Sime-Ngando, 2010).  
We are aware of all the assumptions made here ((i) conversion factors, (ii) *in situ* estimates of  
2310 alkaline phosphatase, (iii) some missing DIP sources in the budget, such as the excretion of  
zooplankton estimated to amount to 22-37% of the phytoP demand at FAST site (Feliú et al.,  
2020), iv) lack of knowledge on the different mechanisms linking P to dust particles, and (iv)

**Supprimé:** We  
**Supprimé:** integrated  
**Supprimé:** that  
**Supprimé:** disappearing  
**Supprimé:** these organisms  
**Supprimé:** \*  
**Supprimé:**  
**Supprimé:** which  
**Supprimé:** indeed  
**Supprimé:** also  
  
**Supprimé:** 2020  
**Supprimé:** that  
  
**Supprimé:** \*  
  
**Supprimé:** however,  
**Supprimé:** allow  
**Supprimé:** as  
**Supprimé:** after

the hypothesis which considers the station as a 1D system. Nevertheless, all these results together suggest that both luxury consumption by Hprok and export via scavenging on mineral particles probably occurred simultaneously and could explain the observed variations of DIP in the ML.

2335

For NO<sub>3</sub>, and in contrast to the observations for DIP, we observed physical exchanges by advection between the ML and NDLb. A N budget within the ML during the period of net NO<sub>3</sub> decrease (between FAST+0.24, and FAST+2.11, Table S2), indicates a net loss of 1343  $\mu\text{mol N m}^{-2}$  within the ML. For this period lasting 1.8 days, the time-integrated phytoN and hprokN demands were 682  $\mu\text{mol N m}^{-2}$  and 378  $\mu\text{mol N m}^{-2}$ , respectively, so that total

2340

biological demand in the ML was 1060  $\mu\text{mol N m}^{-2}$ . During this period, the possible N sources used were disappearing stocks of NO<sub>3</sub> (net diminution assumed to be consumption = 1343  $\mu\text{mol N m}^{-2}$ ), as well as N<sub>2</sub> fixation and *in situ* aminopeptidase activity where fluxes integrated over this time period were 13 and 87  $\mu\text{mol N m}^{-2}$ , respectively. In total, the possible source of N amounted to 1443  $\mu\text{mol N m}^{-2}$ . Keeping in mind that the same potential caveats pointed to DIP (see above) also apply for the calculation of N budget, the biological N demand appeared lower than the sources (difference ~380  $\mu\text{mol N m}^{-2}$ ). On the other hand, at FAST site, vertical advective fluxes of NO<sub>3</sub> from ML to NDLb were up to 337  $\mu\text{mol N m}^{-2} \text{ d}^{-1}$  (Fig. 4), i.e. ~600  $\mu\text{mol N m}^{-2}$  was lost from the ML over 1.8 days. From these two different approaches, exported NO<sub>3</sub> should range between 380 and 600  $\mu\text{mol N m}^{-2}$  over this period.

2350

Thus, about 40% of the NO<sub>3</sub> accumulated in the ML after the rain was likely exported by vertical advection to the NDLb. Organisms present in the DCM could benefit of this input of new nutrients. Indeed, PP and abundances of all 4 phytoplankton groups (*Synechococcus*, *Prochlorococcus*, nano and picoeukaryotes) increased at the DCM after 24h and remained high for 2 days, after the rain event (Fig. S3). The increase in abundances were higher for prokaryotic phytoplankton abundances, as such organisms would likely benefit from their small size and their ability to use DON/DOP organic molecules (Yelton et al., 2016).

2355

## 5. Conclusions

2360

This study reports for the first time, in the context of an oceanographic cruise, simultaneous sampling of atmospheric and ocean biogeochemical parameters to characterize *in situ* the biogeochemical responses to atmospheric deposition within the ML. High-frequency sampling, in particular at the FAST site, confirmed the transitory state of exchanges between

**Supprimé:** ing

**Supprimé:** ,

**Supprimé:** likely

**Supprimé:** to

**Supprimé:** opposition

**Supprimé:** Indeed, NO<sub>3</sub> was higher within the ML than within the NDLb at FAST+0.24 and FAST+0.53 and then NO<sub>3</sub> was lower within the ML than within NDLb at FAST+1.05 and FAST+2.11, suggesting a rapid transfer of NO<sub>3</sub> in the NDLb.

**Supprimé:** s for DIP, we made an

**Supprimé:** from 1520 ; 1113; 852 and to 177  $\mu\text{mol N m}^{-2}$

**Supprimé:** at

**Supprimé:** FAST+0.5, FAST+1.05

**Supprimé:** respectively

**Supprimé:** . This

**Supprimé:** in 1.8 days

**Supprimé:** Over these

**Supprimé:** disappearing

**Supprimé:** which

**Supprimé:** that

**Supprimé:** of time

**Supprimé:** i.e. a total

**Supprimé:** for

**Supprimé:** also

**Supprimé:** thus

**Mis en forme :** Non Exposant/ Indice

**Supprimé:** during

**Supprimé:** that

**Supprimé:** We could conclude that

**Supprimé:** one third

**Supprimé:** T

**Supprimé:** could thus benefit organisms present at the DCM

**Supprimé:** , 1 or 2 days

**Supprimé:** and PP recovered its initial value before rain

**Supprimé:** s

**Mis en forme :** Police :Italique

**Supprimé:** -

**Supprimé:** ,

**Supprimé:** in the context of an oceanographic cruise,

**Supprimé:** dust

**Supprimé:** long duration

**Supprimé:** transient status

2410 the ML and the NDLb. Even if dry deposition measured along the transect was homogeneous and amongst in the lowest observed in the MS, that input could represent up to 121% of the hprokN demand. Furthermore, the signature of the dust wet deposition event on DIP and DIN concentrations was clearly emphasized, considering both the local rain fluxes and the horizontal oceanic mixing of water masses affected by the rain front. Finally, a comparison

2415 with the mesocosms results (where the fertilization is more important due to high dust concentrations) is hard to extrapolate with the data presented here.

2420 Our results have shown the important role played by the ML in the biogeochemical and physical processes responsible for transfers of matter and nutrients between the atmosphere and the nutrient depleted layer below. Thanks to the use of the LWCC technique and access to nanomolar variations of NO<sub>3</sub> and DIP in repeated CTD casts, it was possible to demonstrate the role of the ML and exchanges of NO<sub>3</sub> from the ML to the NDLb by vertical advection when variations of MLD occurred simultaneously to transitory accumulation of NO<sub>3</sub> after a deposition event. The time sequence occurring after a wet dust deposition event was summarized Fig. 6: accumulation of NO<sub>3</sub> in the ML, advection to NDLb, luxury

2425 consumption of DIP by hprok and delayed peaks of DIP, decrease of primary production and its recovery after 2 days mainly visible in the nutrient depleted layer. The effect of dust deposition is a complex and time-controlled trophic cascade within the microbial food web.

2430 Our study shows the important role of intermittent, but strong abiotic effects such as downwelling advection fluxes from the ML to the nutrient depleted layers. It will be important to consider these aspects on budgets and non-stoichiometric models, especially when climate and anthropogenic changes are predicted to increase aerosol deposition in the Mediterranean Sea.

### Data availability

Guieu et al., Biogeochemical dataset collected during the PEACETIME cruise, SEANOE.

2435 [https://doi.org/10.17882/75747 \(2020\)](https://doi.org/10.17882/75747).

### Author contribution

CG and KD designed the study. FVW measured ectoenzymatic activity and BP, AE managed the TAA analysis and treatments, EP measured DIP with the LWCC technique, 2440 CR measured nitrogen fixation, VT assisted in CTD operations and analyzed water

**Supprimé:** layers

**Supprimé:** during

**Supprimé:** cruise

**Supprimé:** ere

**Supprimé:**

**Supprimé:** record

**Supprimé:** Mediterranean

**Supprimé:** r

**Supprimé:** ached

**Supprimé:** , the dust wet deposition event, as usual, was intermittent and patchy in space and time and we caught only one part of the deposition. We hypothesized a fully non-stationary and purely vertical evolution of the oceanic response, lasting for a few days (48 h occupation of the FAST site) and spanning over 40 - 50 km. Under these assumptions, we assume our sampling representative of a wider-ranging water mass than the one crossed by the vessel, integrating every local patch of rain event (rather than only the one received onboard) thanks to horizontal oceanic stirring

**Supprimé:** the

**Supprimé:** ones

**Supprimé:** Nevertheless, o

**Supprimé:** ed

**Supprimé:** s

**Supprimé:** depth

**Supprimé:** after

**Supprimé:** As pictured on Fig. 7, this study confirms previous evidence that hprok in the ML and the presence of dust particles and mechanism of sinking adsorption/desorption play together a role in the transfer of new P from atmospheric deposition from the ML to the nutrient depleted layer. Our results also show the

**Supprimé:** thus

**Supprimé:** ly

**Supprimé:** It

**Supprimé:** ed

**Supprimé:** ed

**Supprimé:** i

**Supprimé:**

**Supprimé:** Underlying research data are being used by researcher participants of the PEACETIME campaign to prepare other papers, and therefore data are not publicly accessible at the time of publication. The data will be accessible (<http://www.obs-yfr.fr/proof/php/PEACETIME/peactime.php> (last access 20/03/2021), once the special issue is completed (all papers should be published by June 2021). The policy of the database is detailed here: <http://www.obs-yfr.fr/proof/php/PEACETIME/peactime.php> ...

masses, JD sampled for DOC and flow cytometry, FVW prepared the ms with contribution from all co-authors.

2520 **Competing interests**

The authors declare that they have no conflict of interest

**Special issue statement**

This article is part of the special issue ‘Atmospheric deposition in the low-nutrient-low-chlorophyll (LNLC) ocean: effects on marine life today and in the future (ACP/BG inter-journal SI)’. It is not associated with a conference.

**Financial support**

The project leading to this publication received funding from CNRS-INSU, IFREMER, CEA, and Météo-France as part of the program MISTRALS coordinated by INSU (doi: 10.17600/17000300) and from the European FEDER fund under project no 1166-39417.

The research of EM was funded by the Spanish Ministry of Science, Innovation and Universities through grant PGC2018-094553B-I00 (POLARIS).

**Supprimé:** Acknowledgements :This study is a contribution of the PEACETIME project (<http://peacetime-project.org>), a joint initiative of the MERMEX and ChArMEx components supported by CNRS-INSU, IFREMER, CEA, and Météo-France as part of the programme MISTRALS coordinated by INSU (doi: 10.17600/17000300).

**Supprimé:** also

**Supprimé:** EACETIME was endorsed as a process study by GEOTRACES and is also a contribution to IMBER and SOLAS international programs.

**Acknowledgements.** This study is a contribution of the PEACETIME project (<http://peacetime-project.org>, last access 07/04/2021), a joint initiative of the MERMEX and ChArMEx components. PEACETIME was endorsed as a process study by GEOTRACES and is also a contribution to IMBER and SOLAS international programs.

The authors thank also many scientists & engineers for their assistance with

2540 sampling/analyses: Samuel Albani for NO<sub>3</sub> nanomolar sampling and Maryline Montanes for NO<sub>3</sub> with LWCC technique, Marc Garel, Sophie Guasco and Christian Tamburini for ectoenzymatic activity, Ruth Flerus and Birthe Zancker for TAA, Joris Guittonneau and Sandra

**Supprimé:** AP and LAP

Nunige for nutrients, Thierry Blasco for POC, Julia Uitz and Céline Dimier for TChl a (analysed at the SAPIG HPLC analytical service at the IMEV, Villefranche), Philippe Catala for flow cytometry analyses, Barbara Marie and Ingrid Obernosterer for DOC analyses and treatments, Sylvain Triquet and Franck Fu for atmospheric particulate nitrogen and phosphorus. Maurizio Ribera d'Alcalá and a second anonymous reviewer helped much to improve this ms.

2565 **References**

Aminot, A., and Kéroutil, R.: Dosage automatique des nutriments dans les eaux marines, in: Méthodes d'analyses en milieu marin, edited by: IFREMER, Plouzané, 188 pp, IBSN no 978-2-7592-0023-8, 2007.

Bardouki, H., Liakakou, H., Economou, C., Sciare, J., Smolik, J., Zdimal, V., Eleftheriadis, K., Lazaridis, M., Dye, C., and Mihalopoulos, N.: Chemical composition of size resolved atmospheric aerosols in the eastern Mediterranean during summer and winter, *Atmos. Environ.*, 37, 195–208, 2003.

Bonnet, S., Grosso, O., and Moutin, T.: Planktonic dinitrogen fixation along a longitudinal gradient across the Mediterranean Sea during the stratified period (BOUM cruise), *Biogeosciences*, 8, 2257–2267, 2011.

Bonnet, S., Caffin, M., Berthelot, H., and Moutin, T.: Hot spot of N<sub>2</sub> fixation in the western tropical South Pacific pleads for a spatial decoupling between N<sub>2</sub> fixation and denitrification, *PNAS letter*, doi: 10.1073/pnas.1619514114, 2017.

Brainerd, K. E., and Gregg, M. C.: Surface mixed and mixing layer depths, *Deep-Sea Research Part I*, 42(9), 1521–1543. doi: 10.1016/0967-0637(95)00068-H, 1995.

Caffin, M., Berthelot, H., Cornet-Barthaux, V., Barani, A., and Bonnet, S.: Transfer of diazotroph-derived nitrogen to the planktonic food web across gradients of N<sub>2</sub> fixation activity and diversity in the western tropical South Pacific Ocean, *Biogeosciences*, 15, 3795–3810, doi: 10.5194/bg-15-3795-2018, 2018.

Carbo, P., Krom, M. D., Homoky, W. B., Benning, L. G., and Herut, B.: Impact of atmospheric deposition on N and P geochemistry in the southeastern Levantine basin, *Deep Sea Res. II*, 52, 3041–3053. doi: 10.1016/j.dsr2.2005.08.014, 2005.

Céa, B., Lefèvre, D., Chirurgien, L., Raimbault, P., Garcia, N., Charrière, B., Grégori, G., Ghiglione, J.-F., Barani, A., Lafont, M., and Van Wambeke, F.: An annual survey of bacterial production, respiration and ectoenzyme activity in coastal NW Mediterranean waters: temperature and resource controls, *Environ. Sci. Pollut. Res.*, doi: 10.1007/s11356-014-3500-9, 2014.

**Supprimé:** .**Supprimé:** -**Supprimé:** .**Supprimé:** .

**Supprimé:** Bressac, M., Wagener, T., Tovar-Sánchez, A., Ridame, C., Albani, S., Fu F., Desboeufs, K. and Guieu C.: Residence time of iron and aluminium in the surface Mediterranean Sea (Peacetime cruise), this special issue, in preparation.

2605 Christaki, U., Courties, C., Massana, R., Catala, P., Lebaron, P., Gasol, J. M., and Zubkov, M.: Optimized routine flow cytometric enumeration of heterotrophic flagellates using SYBR Green I, Limnol. Oceanogr. Methods, 9, doi: 10.4319/lom.2011.9.329, 2011.

Cullen, J. J., Franks, P. J., Karl, D. M., and Longhurst, A. L. A. N.: Physical influences on marine ecosystem dynamics. The sea, 12, 297-336, 2002.

2610 de Boyer Montegut, C., Madec, G., Fisher, A. S., Lazar, A., and Iudicone, D.: Mixed layer depth over the global ocean: An examination of profile data and a profile-based climatology, Journal of Geophysical Research. Oceans, 109, C12003, doi: 10.1029/2004JC002378, 2004.

2615 Delmont, T.O., Quince, C., Shaiber, A., Esen, Ö.C., Lee, S.T.M., Rappé, M.R., McLellan, S.L., Lücker, S. and Murat Eren, A.: Nitrogen-fixing populations of Planctomycetes and Proteobacteria are abundant in surface ocean metagenomes, Nature Microbiology, doi: 10.1038/s41564-018-0176-9, 2018.

Desboeufs, K.: Nutrients atmospheric deposition and variability, in: Atmospheric Chemistry and its Impacts in the Mediterranean Region (ChArMex book), Springer, in press.

2620 Desboeufs, K., Bon Nguyen, E., Chevaillier, S., Triquet, S., and Dulac, F.: Fluxes and sources of nutrient and trace metal atmospheric deposition in the northwestern Mediterranean, Atmospheric Chemistry and Physics, 18, 14477–14492, doi: 10.5194/acp-18-14477-2018, 2018.

2625 Desboeufs, K., Fu, F., Breassac, M., Tovar-Sánchez, A., Triquet, S., Doussin, J-F., Giorio, C., Siour, G., Rodriguez-Romero, A., Wagener, T., Dulac, F., and Guieu, C.: Wet deposition of nutrients and trace metals in the remote Western and central Mediterranean Sea: A source for marine biosphere?, Atmos. Phys. Chem., this special issue, in preparation.

Dittmar, T.H., Cherrier, J. and Ludwichowski, K.-U: The analysis of amino acids in seawater. In: Practical Guidelines for the Analysis of Seawater, edited by: Wurl, O., Boca Raton, FL: CRC-Press, 67–78, 2009.

2630 D'Ortenzio, F., Iudicone, D., de Boyer Montegut, C., Testor, P., Antoine, D., Marullo, S., Santolieri, R., and Madec, G.: Seasonal variability of the mixed layer depth in the

Supprimé: .

Supprimé: Desboeufs, K., Doussin, J.-F., Giorio, C., Triquet, S., Fu, Y., Dulac, F., Garcia-Nieto, D., Chazette, P., Féron, A., Formenti, P., Gaimoz, C., Maisonneuve, F., Riffault, V., Saiz-López, A., Siour, G., Zapf, P., and Guieu, C.: ProcEss studies at the Air-sEa Interface after dust deposition in the MEditerranean sea (PEAcEtIME) cruise: Atmospheric overview, this special issue, in preparation.

2645 | Mediterranean Sea as derived from in situ profiles., Geophysical Research Letters, 32, L12605, doi:10.1029/2005GL022463, 2005.

**Supprimé:** Mediterranean

Djaoudi, K., Van Wambeke, F., Barani, A., Hélias-Nunige, S., Sempéré, R., and Pulido-Villena, E.: Atmospheric fluxes of soluble organic C, N, and P to the Mediterranean Sea: potential biogeochemical implications in the surface layer, *Progress in Oceanography*, 163: 59-69, MERMEX special issue, doi: 2650 | 10.1016/j.pocean.2017.07.008, 2017.

Djaoudi, K., Van Wambeke, F., Coppola, L., D'ortenzio, F., Helias-Nunige, S., Raimbault, P., Taillandier, V., Testor, P., Wagener, T., and Pulido-Villena, E.: Sensitive determination of the dissolved phosphate pool for an improved resolution of its vertical variability in the surface layer: New views in the P-depleted Mediterranean Sea, *Frontiers in Marine Science*, vol 5, article 234, doi: 10.3389/fmars.2018.00234, 2018.

2655 | Djaoudi, K., Van Wambeke, F., Barani, A., Bhaiy, N., Chevaillier, S., Desboeufs, K., Nunige, S., Labiad, M., Henry des Tureaux, T., Lefèvre, D., Nouara, A., Panagiotopoulos, C., Tedetti, M., and Pulido-Villena E.: Potential bioavailability of organic matter from atmospheric particles to marine heterotrophic bacteria, *Biogeosciences*, 17, 6271–6285, <https://doi.org/10.5194/bg-17-6271-2020>, 2020.

**Supprimé:** Lefèvre

**Supprimé:** Experimental evidence of the

**Supprimé:** potential

**Supprimé:** for

**Supprimé:** of aerosols organic matter

**Supprimé:** Biogeosciences Discuss., bg-2020-187, 2020.

**Supprimé:** .

Du, C., Liu, Z., Kao, S.-J., and Dai, M.: Diapycnal fluxes of nutrients in an oligotrophic oceanic regime: The South China Sea, *Geophysical Research Letters*, 44, 11, 510–11, 518, doi: 10.1002/2017GL074921, 2017.

2665 | Feliú, G., Pagano, M., Hidalgo, P., and Carlotti, F.: Structure and function of epipelagic mesozooplankton and their response to dust deposition events during the spring PEACETIME cruise in the Mediterranean Sea, *Biogeosciences*, 17, 5417–5441, <https://doi.org/10.5194/bg-17-5417-2020>, 2020.

2670 | Flaten, G. A., Skjoldal, E. F., Krom, M. D., Law, C. S., Mantoura, F. C., Pitta, P., Psarra, S., Tanaka, T., Tselepides, A., Woodward, E. M., Zohary, T., and Thingstad, T. F.: Studies of the microbial P-cycle during a Lagrangian phosphate-addition experiment in the Eastern Mediterranean, *Deep-Sea Res II*, 52, 2928–2943, 2005.

**Supprimé:** Structure and functioning of epipelagic mesozooplankton and response to dust events during the spring PEACETIME cruise in the Mediterranean Sea, Biogeosciences Discuss., <https://doi.org/10.5194/bg-2020-126>

**Supprimé:**

Fu, F., Desboeufs, K., Triquet, S., Doussin, J-F., Giorio, C., Dulac, F., and Guieu, C.: Solubility and sources of trace metals and nutrients associated with aerosols collected

during cruise PEACETIME in the Mediterranean Sea, *Atmos. Phys. Chem.*, this special issue, in preparation.

**Supprimé:** a

2695 Galletti, Y., Becagli, S., di Sarra, A., Gonnelli, M., Pulido-Villena, E., Sferlazzo, D. M.,  
Traversi, R., Vestri, S., and Santinelli, C.: Atmospheric deposition of organic matter at a  
remote site in the Central Mediterranean Sea: implications for marine ecosystem,  
*Biogeosciences*, 17, 3669–3684, <https://doi.org/10.5194/bg-17-3669-2020>, 2020.

**Supprimé:** Fu, F., Triquet, S., Tovar-Sánchez, A., Bressac, M., Doussin, J.-F., Giorio C., Dulac, F., Guieu, C. and Desboeufs K. : Wet deposition of nutrients and trace metals in the Western and Central Mediterranean Sea: Background rain vs Rain dust, *Atmos. Phys. Chem.*, this special issue, in preparation b.¶

Gardner, W. D., Chung, S. P., Richardson, M. J., and Walsh, I. D.: The oceanic mixed-layer pump, *Deep-Sea Research II* 42, 757-775, 1995.

**Supprimé:** .

2700 Gasol, J. M., and del Giorgio, P. A.: Using flow cytometry for counting natural planktonic bacteria and understanding the structure of planktonic bacterial communities, *Scientia Marina*, 64, 197–224, 2000.

**Supprimé:** -

Gazeau, F., Van Wambeke, F., Marañon, E., Pérez-Lorenzo, M., Alliouane, S., Stolpe, C., Blasco, T., Leblond, N., Zäncker B., Engel A., Marie, B., Dinasquet, J., and Guieu, C.: Impact of dust addition on the metabolism of Mediterranean plankton communities and carbon export under present and future conditions of pH and temperature, *Biogeosciences Discuss. [preprint]*, <https://doi.org/10.5194/bg-2021-20>, in review, 2021.

**Supprimé:**

**Supprimé:** Van Wambeke F.,

**Supprimé:** Ridame C

**Supprimé:** Pérez-Lorenzo M., Barbara Marie, Engel A., Zäncker B., &

**Supprimé:** enrichment on carbon budget and

**Supprimé:** this special issue, in preparation.

2710 Godwin, C. M., and Cotner, J. B.: Aquatic heterotrophic bacteria have highly flexible phosphorus content and biomass stoichiometry, *the ISME Journal*, 9, 2324–2327, doi:10.1038/ismej.2015.34, 2015.

**Supprimé:** -

Guieu, C., and Ridame, C.: Impact of atmospheric deposition on marine chemistry and biogeochemistry, in: *Atmospheric Chemistry and its Impacts in the Mediterranean Region* (ChArMex book), Springer, in press.

**Supprimé:** .

2715 Guieu, C., Dulac, F., Desboeufs, K., Wagener, T., Pulido-Villena, E., Grisoni, J.-M., Louis, J., Ridame, C., Blain, S., Brunet, C., Bon Nguyen, E., Tran, S., Labiad, M., and Dominici, J.-M.: Large clean mesocosms and simulated dust deposition: a new methodology to investigate responses of marine oligotrophic ecosystems to atmospheric inputs, *Biogeosciences*, 7, 2765–2784, doi: 10.5194/BG-7-2765-2010, 2010.

**Supprimé:** -

Guieu, C., Aumont, O., Paytan, A., Bopp, L., Law, C. S., Mahowald, N., Achterberg, E. P.,  
Marañón, E., Salihoglu, B., Crise, A., Wagener, T., Herut, B., Desboeufs, K.,  
2745 Kanakidou, M., Olgun, N., Peters, F., Pulido-Villena, E., Tovar-Sanchez, A., and  
Völker, C.: The significance of episodicity in atmospheric deposition to Low Nutrient  
Low Chlorophyll regions, *Global Biogeochem. Cycles*, 28, 1179–1198,  
doi:10.1002/2014GB004852, 2014a.

Guieu, C., Ridame, C., Pulido-Villena, E., Bressac, M., Desboeufs, K., and Dulac, F.: Impact  
2750 of dust deposition on carbon budget: a tentative assessment from a mesocosm approach,  
*Biogeosciences*, 11, 5621–5635, doi: 10.5194/bg-11-5621-2014, 2014b.

Supprimé: -

Guieu, C., D'Ortenzio, F., Dulac, F., Taillandier, V., Doglioli, A., Petrenko, A., Barrillon, S.,  
Mallet, M., Nabat, P., and Desboeufs, K.: Process studies at the air-sea interface after  
atmospheric deposition in the Mediterranean Sea: objectives and strategy of the  
2755 PEACETIME oceanographic campaign (May–June 2017), *Biogeosciences*, 17, 1–23,  
2020, doi: 10.5194/bg-17-1-2020.

Heimbürger, A., Losno, R., Triquet, S., Dulac F., and Mahowald, N. M.: Direct measurements  
of atmospheric iron, cobalt and aluminium-derived dust deposition at Kerguelen  
Islands, Global Biogeochem. Cy., 26, GB4016, doi:10.1029/2012GB004301, 2012.

2760 Hersbach, H., Bell, B., Berrisford, P., Biavati, G., Horányi, A., Muñoz Sabater, J., Nicolas, J.,  
Peubey, C., Radu, R., Rozum, I., Schepers, D., Simmons, A., Soci, C., Dee, D.,  
Thépaut, J-N.: ERA5 hourly data on single levels from 1979 to present. Copernicus  
Climate Change Service (C3S) Climate Data Store (CDS). doi: 10.24381/cds.adbb2d47,  
2018.

2765 Herut, B., Zohary, T., Krom, M. D., Mantoura, R. F. C., Pitta, P., Psarra, S., Rassoulzadegan,  
F., Tanaka, T. and Thingstad, T. F.: Response of East Mediterranean surface water to  
Saharan dust: On-board microcosm experiment and field observations, *Deep-Sea  
Research II* 52 (2005) 3024–3040, 2005.

2770 Herut, B., Rahav, E., Tsagarakis, T. M., Giannakourou, A., Tsiola, A., Psarra, S., Lagaria, A.,  
Papageorgiou, N., Mihalopoulos, N., Theodosi, C. N., Violaki, K., Stathopoulou, E.,  
Scoullos, M., Krom, M. D., Stockdale, A., Shi, Z., Berman-Frank, I., Meador, T. B.,  
Tanaka, T., and Paraskevi, P.: The potential impact of Saharan dust and polluted

aerosols on microbial populations in the East Mediterranean Sea, an overview of a  
2775 mesocosm experimental approach, *Front. Mar. Sci.*, 3, 226, doi:  
10.3389/fmars.2016.00226, 2016.

Hoppe, H.-G., Ducklow, H., and Karrasch, B.: Evidence for dependency of bacterial growth  
on enzymatic hydrolysis of particulate organic matter in the mesopelagic ocean, *Mar.  
Ecol. Prog. Ser.*, 93, 277–283, 1993.

**Supprimé:** Holmes, R. M., Aminot, A., Kérout, R., Hooker, B. A., and Peterson, B. J.: A simple and precise method for measuring ammonium in marine and freshwater ecosystems, *Can. J. Fish. Aquat. Sci.*, 56, 1801–1808, 1999.

**Supprimé:** -

2780 Ibello, V., Cantoni, C., Cozzi, S., and Civitarese, G.: First basin-wide experimental results on  
N2 fixation in the open Mediterranean Sea, *Geophys. Res. Lett.*, 37, L03608,  
doi:10.1029/2009GL041635, 2010.

Izquierdo, R., Benítez-Nelson, C. R., Masqué, P., Castillo, S., Alastuey, A., and Àvila, A.:  
Atmospheric phosphorus deposition in a near-coastal rural site in the NE Iberian  
2785 Peninsula and its role in marine productivity, *Atmos. Environ.*, 49, 361–370, doi:  
10.1016/j.atmosenv.2011.11.007, 2012.

Jumars, P. A., Penry, D. L., Baross, J. A., Perry, M. A., and Frost, B. W.: Closing the  
microbial loop : dissolved carbon pathway to heterotrophic bacteria from incomplete  
ingestion, digestion and absorption in animals, *Deep-Sea Research*, 483–495, 1989.

**Supprimé:** -

2790 Kamykowski, D., and Zentara, S. J.: Nitrate and silicic acid in the world ocean: Patterns and  
processes, *Mar. Ecol. Prog. Ser.*, 26, 47–59, 1985.

Kanakidou, M., Myriokefalitakis, S., and Tsigaridis, K.: Aerosols in atmospheric chemistry  
and biogeochemical cycles of nutrients, *Environ. Res. Lett.*, 13, 063004, doi:  
10.1088/1748-9326/aabedb, 2018.

2795 Kanakidou, M., Myriokefalitakis, S., and Tsagkaraki, M.: Atmospheric inputs of nutrients to  
the Mediterranean Sea, *Deep Sea Research Part II: Topical Studies in Oceanography*,  
171, 104606, doi: 10.1016/j.dsr2.2019.06.014, 2020.

Kirchman, D. L.: Leucine incorporation as a measure of biomass production by heterotrophic  
bacteria, in: *Handbook of methods in aquatic microbial ecology*, edited by : Kemp, P.F.,  
2800 Sherr, B.F., Sherr, E.B., and Cole, J.J., Lewis, Boca Raton, 509–512, 1993.

**Supprimé:**

**Supprimé:** .

**Supprimé:** I

Kouvarakis, G., Mihalopoulos, N., Tselepidis, T., and Stavrakakis, S.: On the importance of atmospheric nitrogen inputs on the productivity of eastern Mediterranean, *Global Biogeochemical Cycles*, 15, 805–818, doi:10.1029/2001GB001399, 2001.

Supprimé: ¶

2815 Krom, M. D., Herut, B., and Mantoura, R. F. C.: Nutrient budget for the eastern Mediterranean: Implication for phosphorus limitation, *Limnol. Oceanogr.*, 49, 1582–1592, doi: 10.4319/lo.2004.49.5.1582, 2004.

Supprimé: Karl, D. M.: Microbially mediated transformations of phosphorus in the sea: New views of an old cycle. *Ann. Rev. Mar. Sci.* 6: 279–337, doi: 10.1146/annurev-marine-010213-135046, 2014. ¶

Supprimé: -

2820 Louis, J., Bressac, M., Pedrotti, M.-L., and Guieu, C.: Dissolved inorganic nitrogen and phosphorus dynamics in sea water following an artificial Saharan dust deposition event, *Frontiers Marine Sci.*, 2, article 27, doi: 10.3389/fmars.2015.00027, 2015.

Supprimé: Krom, M. D., Emeis, K.-C., and Van Capellen, P.: Why is the eastern Mediterranean phosphorus limited? *Progress In Oceanography*, 85, 236–244, 2010. ¶

Lindroth, P., and Mopper, K.: High performance liquid chromatographic determination of sub picomole amounts of amino acids by precolumn fluorescence derivatization with o-phthalidialdehyde, *Anal. Chem.* 51, 1667–1674, 1979. ¶

Supprimé: -

Løvdal, T., Skjoldal, E. F., Heldal, M., Norland, S., and Thingstad, T. F.: Changes in Morphology and Elemental Composition of *Vibrio splendidus* Along a Gradient from Carbon-limited to Phosphate-limited Growth, *Microb. Ecol.*, 55, 152–161, doi: 10.1007/s00248-007-9262-x, 2008.

2825 Makino, W., Cotner, J. B., Sterner, R. W., and Elser, J. J.: Are bacteria more like plants or animals? Growth rate and resource dependence of bacterial C : N : P stoichiometry, *Functional Ecology*, 17, 121–130, 2003.

Supprimé: -

2830 Malits, A., Cattaneo, R., Sintes, E., Gasol, J. M., Herndl, G. J., and Weinbauer, M.: Potential impacts of black carbon on the marine microbial community, *Aquat Microb Ecol.*, 75, 27–42, doi: 10.3354/ame01742, 2015.

Supprimé: -

2835 Marañón, E., Fernández, A., Mouríño-Carballido, B., Martínez-García, S., Teira, E., Cermeño, P., Chouciño, P., Huete-Ortega, M., Fernández, E., Calvo-Díaz, A., Morán, X. A. G., Bode, A., Moreno-Ostos, E., Varela, M. M., Patey, M. D., and Achterberg, E. P.: Degree of oligotrophy controls the response of microbial plankton to Saharan dust, *Limnology and Oceanography*, 55, 2339–2352, 2010.

Supprimé: -

Supprimé: -

2840 Marañón, E., Van Wambeke, F., Uitz, J., Boss, E. S., Dimier, C., Dinasquet, J., Angel, A., Haëntjens, N., Pérez-Lorenzo, M., Taillardier, V., and Zäncker, B.: Deep maxima of phytoplankton biomass, primary production and bacterial production in the Mediterranean Sea, *Biogeosciences*, 18, 1749–1767, doi:10.5194/bg-18-1749-2021, 2021.

Supprimé: Dinasquet, J., Haëntjens, N., Dimier, C.,

Supprimé: during late spring

Supprimé: Discuss.

Supprimé: -

Supprimé: in review, bg 2020-261, 2020

2875 Mari, X., Guinot, B., Chu, V. T., Brune, J., Lefebvre, J.-P., Pradeep Ram, A. S., Raimbault, P., Dittmar, T., and Niggemann, J.: Biogeochemical Impacts of a Black Carbon Wet Deposition Event in Halong Bay, Vietnam, *Front. Mar. Sci.*, 6, article 185, doi: 10.3389/fmars.2019.00185, 2019.

2880 Marie, D., Simon, N., Guillou, L., Partensky, F., and Vaulot, D.: Flow Cytometry Analysis of Marine Picoplankton, in: *In Living Color: Protocols in Flow Cytometry and Cell Sorting*, edited by: Diamond, R. A., and Demaggio, S., Springer, Berlin, Heidelberg, 421–454, 2000.

Supprimé: -

2885 Markaki, Z., Loyer-Pilot, M. D., Violaki, K., Benyahya, L., and Mihalopoulos, N.: Variability of atmospheric deposition of dissolved nitrogen and phosphorus in the Mediterranean and possible link to the anomalous seawater N/P ratio, *Marine Chemistry*, 120, 187–194, doi: 10.1016/j.marchem.2008.10.005, 2010.

Supprimé: -

2890 Martiny, A. C., Pham, C. T. A., Primeau, F. W., Vrugt, J. A., Moore, J. K., Levin, S. A., and Lomas, M. W.: Strong latitudinal patterns in the elemental ratios of marine plankton and organic matter, *Nature geosciences*, 6, 279–283, doi: 10.1038/ngeo1757, 2013.

Supprimé: -

Mermex Group.: Marine ecosystems' responses to climatic and anthropogenic forcings in the Mediterranean, *Progress in Oceanography*, 91, 97–166, doi: 10.1016/j.pocean.2011.02.003, 2011.

Supprimé: -

2895 [Mescioglu E., Rahav E., Frada M.J., Rosenfeld S., Raveh O., Galletti Y., Santinelli C., Herut B., Paytan A.: Dust-associated airborne microbes affect primary and bacterial production rates, and eukaryote diversity, in the Northern Red Sea: A mesocosm approach. \*Atmosphere\*, 10, article 358, https://doi.org/10.3390/atmos10070358, 2019.](#)

Moreno, A. R., and Martiny, A. C.: Ecological stoichiometry of ocean plankton, *Ann. Rev. Mar. Sci.*, 10, 43–69, 2018.

Supprimé: -

2900 Moutin, T., and Prieur, L.: Influence of anticyclonic eddies on the Biogeochemistry from the Oligotrophic to the Ultraoligotrophic Mediterranean (BOUM cruise), *Biogeosciences*, 9 (10), 3827–3855, doi: 10.5194/bg-9-3827-2012, 2012.

Supprimé: .

Supprimé: pp.

Supprimé: -

Supprimé: .

Supprimé: -

Orsini, D., Ma, Y., Sullivan, A., Sierau, B., Baumann, K., and Weber, R.: Refinements to the Particle-Into-Liquid Sampler (PILS) for Ground and Airborne Measurements of Water Soluble Aerosol Composition, *Atmospheric Environment*, 37, 1243–1259, 2003.

2915 Omand, M. M. and Mahadevan, A.: The shape of the oceanic nitracline, *Biogeosciences*, 12, 3273–3287, doi: 10.5194/bg-12-3273-2015, 2015.

Pujo-Pay, M., and Raimbault, P.: Improvements of the wet-oxidation procedure for simultaneous determination of particulate organic nitrogen and phosphorus collected on filters, *Mar. Ecol. Prog. Ser.*, 105, 203–207, 1994.

2920 Pradeep Ram, A. S., and Sime-Ngando, T.: Resources drive trade-off between viral lifestyles in the plankton: evidence from freshwater microbial microcosms, *Environ Microbiol*, 12, 467–479, doi: 10.1111/j.1462-2920.2009.02088.x, 2010.

Pulido-Villena, E., Wagener, T., and Guieu, C.: Bacterial response to dust pulses in the western Mediterranean: Implications for carbon cycling in the oligotrophic ocean, *Global Biogeochem. Cycles*, 22, GB1020, doi:10.1029/2007GB003091, 2008.

2925 Pulido-Villena, E., Rérolle, V., and Guieu, C.: Transient fertilizing effect of dust in P-deficient surface LNLC ocean. *Geophysical Research Letters*, 37, L01603, doi:10.1029/2009GL041415, 2010.

Pulido-Villena, E., Baudoux, A.-C., Obernosterer, I., Landa, M., Caparros, J., Catala, P., Georges, C., Harmand, J., and Guieu, C.: Microbial food web dynamics in response to a Saharan dust event: results from a mesocosm study in the oligotrophic Mediterranean Sea, *Biogeosciences*, 11, 337–371, 2014.

2930 Pulido-Villena, E., Desboeufs, K., Djaoudi, K., Van Wambeke, F., Barrillon, S., Doglioli, A., Petrenko, A., TAILLANDIER, V., Fu, Y., Gaillard, T., Guasco, S., Nunige, S., Triquet, S., and Guieu, C.: Phosphorus cycling in the upper waters of the Mediterranean Sea (Peacetime cruise): relative contribution of external and internal sources, *Biogeosciences Discuss.*, [preprint], <https://doi.org/10.5194/bg-2021-94>, in review, 2021.

Supprimé: -

Supprimé: -

Supprimé: -

Supprimé: ¶  
Pulido-Villena, E., Van Wambeke, F., Desboeufs, K., Petrenko, A., Barrillon, S., Djaoudi, K., Doglioli, A., D'Ortenzio, F., Fu, Y., Gaillard, T., Guasco, S., Nunige, S., Raimbault, P., TAILLANDIER, V., Triquet, S., and Guieu, C.: Phosphorus cycling in the upper waters of the Mediterranean Sea (Peacetime cruise): relative contribution of external and internal sources, this special issue, in preparation. ¶

Déplacé vers le bas [1]: Pulido-Desboeufs, K., Petrenko, A., Barrillon, S., Djaoudi, K., Doglioli, A., D'Ortenzio, F., Fu, Y., Gaillard, T., Guasco, S., Nunige, S., Raimbault, P., TAILLANDIER, V., Triquet, S., and Guieu, C.: Phosphorus cycling in the upper waters of the Mediterranean Sea (Peacetime cruise): relative contribution of external and internal sources, this special issue, in preparation. ¶

Supprimé: .

Supprimé: -

Déplacé (insertion) [1]

Supprimé: Desboeufs, K.,

Supprimé: ., Barrillon, S., Djaoudi, K.

Supprimé:

Supprimé: Doglioli, A., D'Ortenzio, F., Fu, Y., Gaillard, T., Guasco, S., Nunige, S., Raimbault, P., TAILLANDIER, V.,

2975 Rahav, E., Herut, B., Levi, A., Mulholland, M. R., and Berman-Frank, I.: Springtime contribution of dinitrogen fixation to primary production across the Mediterranean Sea. *Ocean Sci.* 9, 489–498. doi: 10.5194/os-9-489-2013, 2013a

Rahav, E., Herut, B., Stambler, N., Bar-Zeev, E. Mulholland, M. R., and Berman-Frank, I.: Uncoupling between dinitrogen fixation and primary productivity in the eastern Mediterranean Sea. *J. Geophys. Res. Biogeosci.*, 118, 195–202, doi:10.1002/jgrg.20023, 2013b.

2980 Rahav, E., Paytan, A., Chien, C.-T., Ovadia, G., Katz, T., and Herut, B.: The Impact of Atmospheric Dry Deposition Associated Microbes on the Southeastern Mediterranean Sea Surface Water following an Intense Dust Storm. *Front. Mar. Sci.* 3, 127, doi: 10.3389/fmars.2016.00127, 2016.

2985 Richon, C., Dutay, J. C., Dulac, F., Wang, R., Balkanski, Y., Nabat, P., Aumont, O., Desboeufs, K., Laurent, B., Guieu, C., Raimbault, P., and Beuvier, J.: Modeling the impacts of atmospheric deposition of nitrogen and desert dust-derived phosphorus on nutrients and biological budgets of the Mediterranean Sea. *Prog. Oceanogr.* 163, 21–39, doi: 10.1016/j.pocean.2017.04.009, 2018.

2990 Ridame, C., Moutin, T., and C. Guieu.: Does phosphate adsorption onto Saharan dust explain the unusual N/P ratio in the Mediterranean Sea? *Oceanologica Acta*, 26, 629–634, doi: 10.1016/S0399-1784(03)00061-6, 2003.

Ridame, C., Le Moal, M., Guieu, C., Ternon, E., Biegala, I., L'Helguen, S., and Pujo-Pay, M.: Nutrient control of N<sub>2</sub> fixation in the oligotrophic Mediterranean Sea and the impact of Saharan dust events. *Biogeosciences*, 8, 2773–2783, doi:10.5194/bg-8-2773-2011, 2011.

2995 Sala, M. M., Peters, F., Gasol, J. M., Pedros-Alio, C., Marrasse, C., and Vaque, D.: Seasonal and spatial variations in the nutrient limitation of bacterioplankton growth in the northwestern Mediterranean. *Aquat. Microb. Ecol.*, 27, 47–56, 2002.

Sandroni, V., Raimbault, P., Migon, C., Garcia, N., and Gouze, E.: Dry atmospheric deposition and diazotrophy as sources of new nitrogen to northwestern Mediterranean oligotrophic surface waters. *Deep-Sea Res. I*, 54, 1859–1870, doi:10.1016/j.dsr.2007.08.004, 2007.

**Supprimé:** this special issue, in preparation. ¶

**Mis en forme :** Retrait : Gauche : 0 cm, Suspendu : 1,27 cm, Espace Avant : 10 pt, Bordure : Haut: (Pas de bordure), Bas: (Pas de bordure), Gauche: (Pas de bordure), Droite: (Pas de bordure), Entre : (Pas de bordure)

**Supprimé:** 2013a

**Supprimé:** ¶  
Rahav, E. Herut, B., Levi, A.,  
Mulholland, M.R., and Berman-Frank,  
I.: Springtime contribution of dinitrogen  
fixation to primary production across the  
Mediterranean Sea. *Ocean Sci.* 9, 489–  
498. doi: 10.5194/os-9-489-2013, 2013b.¶

**Supprimé:** -

**Supprimé:**

**Supprimé:** -

**Supprimé:** M.

**Supprimé:** C

**Supprimé:** E

**Supprimé:** I. C.

**Supprimé:** S.

**Supprimé:** M.

**Supprimé:** .

**Supprimé:** -

**Supprimé:** Ridame C., Dinasquet J.,  
Bigeard E., Hallstrom, S., Riemann  
L., Tovar-Sanchez A., Gazeau F.,  
Baudoux A-C., Guieu C., Impact of dust  
enrichment on N2 fixation and diversity  
of diazotrophs under present and future  
conditions of pH and temperature, this  
special issue, in preparation.¶

**Supprimé:** -

Taillardier, V., Prieur, L., D'Ortenzio, F., Ribera d'Alcalà, M., and Pulido-Villena, E.:  
 3035 Profiling float observation of thermohaline staircases in the western Mediterranean Sea  
 and impact on nutrient fluxes, *Biogeosciences*, 17, 3343–3366, 2020.

Talarmin A, Van Wambeke F., Lebaron P., and Moutin T.: Vertical partitioning of phosphate  
 uptake among picoplankton groups in the low Pi Mediterranean Sea, *Biogeosciences*,  
 12: 1237–1247 doi:10.5194/bg-12-1237-2015, 2015.

3040 Tanaka, T., Thingstad, T. F., Christaki, U., Colombe, J., Cornet-Barthaux, V., Courties, C.,  
 Grattepanche, J.-D., Lagaria, A., Nedoma, J., Oriol, L., Psarra, S., Pujo-Pay, M., and  
 Van Wambeke, F.: Lack of P-limitation of phytoplankton and heterotrophic prokaryotes  
 in surface waters of three anticyclonic eddies in the stratified Mediterranean Sea,  
*Biogeosciences*, 8, 525–538, doi: 10.5194/bg-8-525-2011, 2011.

3045 Tovar-Sánchez, A., Rodríguez-Romero, A., Engel, A., Zäncker, B., Fu, F., Marañón, E., Pérez-Lorenzo, M., Bressac, M., Wagener, T., Triquet, S., Siour, G., Desboeufs, K., and Guieu, C.: Characterizing the surface microlayer in the Mediterranean Sea: trace metal concentrations and microbial plankton abundance, *Biogeosciences*, 17, 2349–2364, <https://doi.org/10.5194/bg-17-2349-2020, 2020>

3050 Thingstad, T., Krom, M. D., Mantoura, F., Flaten, G., Groom, S., Herut, B., Kress, N., Law, C. S., Pasternak, A., Pitta, P., Psarra, S., Rassoulzadegan, F., Tanaka, T., Tselepides, A., Wassmann, P., Woodward, M., Riser, C., Zodiatis, G., and Zohary, T.: Nature of phosphorus limitation in the ultraoligotrophic eastern Mediterranean, *Science*, 309, 1068–1071, doi: 10.1126/science.1112632, 2005.

3055 Van Wambeke, F., Christaki, U., Giannakourou, A., Moutin, T., and Souvmerzoglou, K.:  
 Longitudinal and vertical trends of bacterial limitation by phosphorus and carbon in  
 the Mediterranean Sea, *Microb. Ecol.*, 43, 119–133, doi: 10.1007/s00248-001-0038-4,  
 2002.

3060 Van Wambeke, F., Gimenez, A., Duhamel, S., Dupouy, C., Lefevre, D., Pujo-Pay, M., and  
 Moutin, T.: Dynamics and controls of heterotrophic prokaryotic production in the  
 western tropical South Pacific Ocean: links with diazotrophic and photosynthetic  
 activity, *Biogeosciences*, 15: 2669–2689, doi: 10.5194/bg-15-2669-2018, 2018.

Supprimé: -

Supprimé: ¶

Supprimé: Thingstad, T. F., and Rassoulzadegan, F.: Nutrient limitations, microbial food webs, and 'biological C-pumps': suggested interactions in a P-limited Mediterranean, *Mar. Ecol. Prog. Ser.*, 117, 299–306, 1995.¶

Supprimé: -

Supprimé: -

Supprimé:

Supprimé:

3075 Van Wambeke, F., Pulido-Villena, E., Catala, P., Dinasquet, J., Djaoudi, K., Engel, A., Garel, M., Guasco, S., Marie, B., Nunige, S., Taillandier, V., Zäncker, B., and Tamburini, C.: Spatial patterns of ectoenzymatic kinetics in relation to biogeochemical properties in the Mediterranean Sea and the concentration of the fluorogenic substrate used, Biogeosciences, 18, 2301-2323, doi:10.5194/bg-18-2301-2021, 2021.

3080 Yelton, A. P., Acinas, S. G., Sunagawa, S., Bork, P., Pedros-Alio, C., Chisholm, S. W.: Global genetic capacity for mixotrophy in marine picocyanobacteria, ISME J 10:2946-2957, 2016.

Zhang, J.-Z., and Chi, J.: Automated analysis of nano-molar concentrations of phosphate in natural waters with liquid waveguide, Environ. Sci. Technol., 36, 1048-1053, doi : 10.1021/es011094v, 2002.

**Supprimé:** s

**Supprimé:** biphasic

**Supprimé:** related

**Supprimé:** Discuss.

**Supprimé:**

**Supprimé:** in review, bg-2020-253, 2020

**Supprimé:** Vincent, J., Laurent, B., Losno, R., Bon Nguyen, E., Roullet, P., Sauvage, S., Chevailler, S., Coddeville, P., Ouboulmane, N., di Sarra, A. G., Tovar-Sánchez, A., Sferlazzo, D., Massanet, A., Triquet, S., Morales Baquero, R., Fornier, M., Coursier, C., Desboeufs, K., Dulac, F., and Bergametti, G.: Variability of mineral dust deposition in the western Mediterranean basin and south-east of France, Atmos. Chem. Phys., 16, 8749-8766, doi: 10.5194/acp-16-8749-2016, 2016.¶

**Supprimé:** .

**Supprimé:**

**Supprimé:** -

**Table 1.** Main biogeochemical features/trophic conditions during the PEACETIME cruise. For TYR, ION and FAST sites investigated over several days, means  $\pm$  sd are indicated. ITChla: Integrated total chlorophyll a (Chla + dvChla). IPP: Integrated particulate primary production; IBP: integrated heterotrophic prokaryotic production. Integrations from surface to 200 m depth for all data expect IPP, integrated down to the depth of 1% Photosynthetically Active Radiation (PAR) level.

**Mis en forme :** Anglais (États-Unis)

**Supprimé:** during

**Mis en forme :** Anglais (États-Unis)

**Supprimé:**

**Supprimé:** from surface to 200 m depth.

|      | sampling date  | Lat. °N  | Long. °E | Temp. at 5 m °C | Bottom depth m | DCM depth m | ITChla mg chla m <sup>-2</sup> | IPP mg C m <sup>-2</sup> d <sup>-1</sup> | IBP mg C m <sup>-2</sup> d <sup>-1</sup> |
|------|----------------|----------|----------|-----------------|----------------|-------------|--------------------------------|--|--|
| ST1  | May 12         | 41°53.5  | 6°20     | 15.7            | 1580           | 49          | 35,0                           | 284                                      | 51                                       |
| ST2  | May 13         | 40°30.36 | 6°43.78  | 17.0            | 2830           | 65          | 32,7                           | 148                                      | 55                                       |
| ST3  | May 14         | 39°08.0  | 7°41.0   | 14.3            | 1404           | 83          | 23,2                           | 140                                      | 77                                       |
| ST4  | May 15         | 37°59.0  | 7°58.6   | 19.0            | 2770           | 64          | 29,2                           | 182                                      | 66                                       |
| ST5  | May 16         | 38°57.2  | 11°1.4   | 19.5            | 2366           | 77          | 30,5                           | 148                                      | 51                                       |
| TYR  | May 17-20      | 39°20.4  | 12°35.56 | 19.6            | 3395           | 80 $\pm$ 6  | 29 $\pm$ 3                     | 170 $\pm$ 35                             | 57 $\pm$ 3                               |
| ST6  | May 22         | 38°48.47 | 14°29.97 | 20.0            | 2275           | 80          | 18,7                           | 142                                      | 62                                       |
| ST7  | May 24         | 36°39.5  | 18°09.3  | 20.6            | 3627           | 87          | 24.2                           | 158                                      | 57                                       |
| ION  | May 25-28      | 35°29.1  | 19°47.77 | 20.6            | 3054           | 97 $\pm$ 5  | 29 $\pm$ 2                     | 208 $\pm$ 15                             | 51 $\pm$ 9                               |
| ST8  | May 30         | 36°12.6  | 16°37.5  | 20.8            | 3314           | 94          | 31.6                           | 206                                      | 71                                       |
| ST9  | June 2         | 38°08.1  | 5°50.5   | 21.2            | 2837           | 91          | 36.1                           | 214                                      | 64                                       |
| FAST | June 2-7 and 9 | 37°56.8  | 2°54.6   | 21.0            | 2775           | 79 $\pm$ 8  | 34 $\pm$ 8                     | 211 $\pm$ 57                             | 92 $\pm$ 11                              |
| ST10 | June 8         | 37°27.58 | 1°34.0   | 21.6            | 2770           | 89          | 28,9                           | nd                                       | 96                                       |

**Table 2.** N budget at the short stations within the surface mixed layer (ML). Integrated stocks (NO<sub>3</sub>,  $\mu\text{mol N m}^{-2}$ ) and fluxes (heterotrophic prokaryotic N demand (hprokN demand), phytoplankton N demand (phytoN demand), in situ leucine aminopeptidase hydrolysis fluxes (LAP), dry atmospheric deposition of NO<sub>3</sub> and NH<sub>4</sub> (all fluxes in  $\mu\text{mol N m}^{-2} \text{ d}^{-1}$ ). Values

3125 presented as mean  $\pm$  sd. SD was calculated using propagation of errors; For hprokN demand

triplicate measurements at each depth and a C/N ratio of  $7.3 \pm 1.6$ ; for phytoN demand

triplicate measurements of PP at each depth and a C/N ratio of  $7 \pm 1.4$ ; for LAP the analytical

TAA error and the V<sub>m</sub> and K<sub>m</sub> errors; for N<sub>2</sub>fix the coefficient of variation was 10% for

volumetric fluxes  $> 0.1 \text{ nmole N l}^{-1} \text{ d}^{-1}$  and 20% for lower values. For dry deposition, sd is

based on the variability of the NO<sub>3</sub> and NH<sub>4</sub> concentrations solubilized from aerosols during

the occupation of the station (see methods section 2.2.1). MLD: mixed layer depth. na: not

3130 available because under LWCC detection limits.

**Supprimé:**

**Supprimé:** of measurements

**Supprimé:** (

**Supprimé:** all data

**Supprimé:** ),

**Supprimé:** (

**Supprimé:** hprokN demand)

**Supprimé:** (phytoN demand)

| stations | MLD | stocks                   | biological fluxes                       |   |   |   | Dry deposition                          |   |
|----------|-----|--------------------------|---|---|---|---|---|---|
|          |     |                          | phytoN demand                           | hprokN demand                           | LAP                                     | N <sub>2</sub> fixation                 | NO <sub>3</sub>                         | NH <sub>4</sub>                         |
|          | m   | $\mu\text{mol N m}^{-2}$ | $\mu\text{mol N m}^{-2} \text{ d}^{-1}$ |
| ST1      | 21  | na                       | 1468 $\pm$ 325                          | 184 $\pm$ 40                            | 121 $\pm$ 28                            | 14.6 $\pm$ 1.5                          | 18.6 $\pm$ 1.4                          | 1.5 $\pm$ 0.3                           |
| ST2      | 21  | na                       | 481 $\pm$ 161                           | 163 $\pm$ 35                            | 48 $\pm$ 24                             | 10.7 $\pm$ 1.1                          | 23.7 $\pm$ 2.2                          | 4.1 $\pm$ 0.9                           |
| ST3      | 11  | na                       | 282 $\pm$ 82                            | 126 $\pm$ 28                            | 40 $\pm$ 17                             | 7.8 $\pm$ 0.8                           | 33.8 $\pm$ 3.6                          | 4.7 $\pm$ 0.5                           |
| ST4      | 15  | na                       | 246 $\pm$ 80                            | 132 $\pm$ 28                            | 83 $\pm$ 20                             | 10.7 $\pm$ 1.1                          | 23.8 $\pm$ 2.9                          | 6.3 $\pm$ 2.6                           |
| ST5      | 9   | 261 $\pm$ 22             | 112 $\pm$ 29                            | 42 $\pm$ 9                              | 17 $\pm$ 12                             | 4.8 $\pm$ 0.5                           | 27.0 $\pm$ 7.5                          | 7.9 $\pm$ 1.8                           |
| ST6      | 18  | 162 $\pm$ 14             | 410 $\pm$ 116                           | 204 $\pm$ 44                            | 48 $\pm$ 24                             | 9.1 $\pm$ 0.9                           | 15.0 $\pm$ 0.6                          | 9.3 $\pm$ 0.7                           |
| ST7      | 18  | 162 $\pm$ 14             | 226 $\pm$ 123                           | 148 $\pm$ 33                            | 83 $\pm$ 18                             | 10.5 $\pm$ 1.1                          | 23.6 $\pm$ 1.9                          | 8.0 $\pm$ 1.2                           |
| ST8      | 14  | 911 $\pm$ 77             | 274 $\pm$ 66                            | 130 $\pm$ 33                            | 25 $\pm$ 8                              | 4.3 $\pm$ 0.5                           | 13.4 $\pm$ 1.7                          | 3.8 $\pm$ 0.6                           |
| ST9      | 7   | 819 $\pm$ 70             | 259 $\pm$ 70                            | 85 $\pm$ 22                             | 21 $\pm$ 6                              | 3.4 $\pm$ 0.4                           | 27.4 $\pm$ 3.8                          | 13.5 $\pm$ 0.8                          |
| ST10     | 19  | 2074 $\pm$ 176           | 495 $\pm$ 31                            | 294 $\pm$ 64                            | 42 $\pm$ 26                             | 13.6 $\pm$ 1.4                          | 23.9 $\pm$ 3.4                          | 4.1 $\pm$ 0.4                           |

3135

**Table 3.** Characteristics and nutrient fluxes estimated in the 2 rains collected during the PEACETIME cruise at ION and FAST sites.

| event                                       | Rain ION         | Rain FAST          |
|---|------------------|--------------------|
| Date and local time                         | 29/05 05:08-6:00 | 05/06 02:36-3:04   |
| <u>Estimated precipitation</u><br>(mm)      | <u>3.5 ± 1.2</u> | <u>5.7 ± 1.4</u>   |
| DIP Flux nmol P m <sup>-2</sup>             | <u>663 ± 227</u> | <u>1146 ± 290</u>  |
| DOP Flux nmol P m <sup>-2</sup>             | <u>974 ± 334</u> | <u>908 ± 230</u>   |
| POP fluxes nmol P m <sup>-2</sup>           | <u>239 ± 82</u>  | <u>8801 ± 2227</u> |
| NO <sub>3</sub> Flux μmol N m <sup>-2</sup> | <u>67 ± 22</u>   | <u>341 ± 86</u>    |
| NH <sub>4</sub> Flux μmol N m <sup>-2</sup> | <u>71 ± 24</u>   | <u>208 ± 53</u>    |
| DIN Flux μmol N m <sup>-2</sup>             | <u>138 ± 47</u>  | <u>550 ± 139</u>   |

**Supprimé:** of

**Supprimé:** The collector surface was 0.045 m<sup>2</sup>

**Supprimé:** 1

**Supprimé:** 2

**Supprimé:** Location

...

**Supprimé:** Duration min

**Supprimé:** 52

**Supprimé:** 28

**Supprimé:** Collected volume ml

...

**Supprimé:** 495.5

**Supprimé:** 129

**Supprimé:** 728.2

**Supprimé:** 103

**Supprimé:** 179

**Supprimé:** 994

**Supprimé:** 50.0

**Supprimé:** 115.7

**Supprimé:** 53.2

**Supprimé:** 70.6

**Supprimé:** 103

**Supprimé:** 187

## Figure legends

**Figure 1.** Nitrate ( $\text{NO}_3$ ) aerosol concentration along the PEACETIME transect. The locations of two rain events are indicated by large black circles. Stations ST 1 to 4 were not sampled for 3175 nutrient analysis at a nanomolar level.

Supprimé: analysis of  
Supprimé: s

**Figure 2.** Representation of the mixed layer (ML), the bottom of the nitrate ( $\text{NO}_3$ ) depleted layer (NDLb), delineated by the nitracline depth and the mixed layer depth (MLD).

Supprimé: cruise

**Figure 3.** a) Evolution of the wind speed during the PEACETIME cruise. The stations are indicated in yellow and dates in black. Vertical dotted lines delineate the beginning and the 3180 end of the ship's deployment at TYR, ION and FAST sites. The two rain events collected on board are indicated in solid vertical red arrows and surrounding observed rain events by horizontal dashed red arrows. b) 0-100 m vertical distribution of nitrate ( $\text{NO}_3$ ) with depth. The MLD (in red) and nitracline (in brown) are indicated.

Supprimé: of occupation  
Supprimé: s

**Figure 4.** Average concentration of nitrate ( $\text{NO}_3$ ) in the ML and the NDLb, and  $\text{NO}_3$  flux 3185 from the ML to NDLb. The stations have been classified into 4 types (1 in blue, 2 in green, 3 in yellow, 4 in red, see section Results and Table S1 for definitions). Error bars are indicated by standard deviation around average values for nitrate concentrations, and error propagation for the flux from ML to NDLb using a 0.5 m uncertainty in the MLD variation.

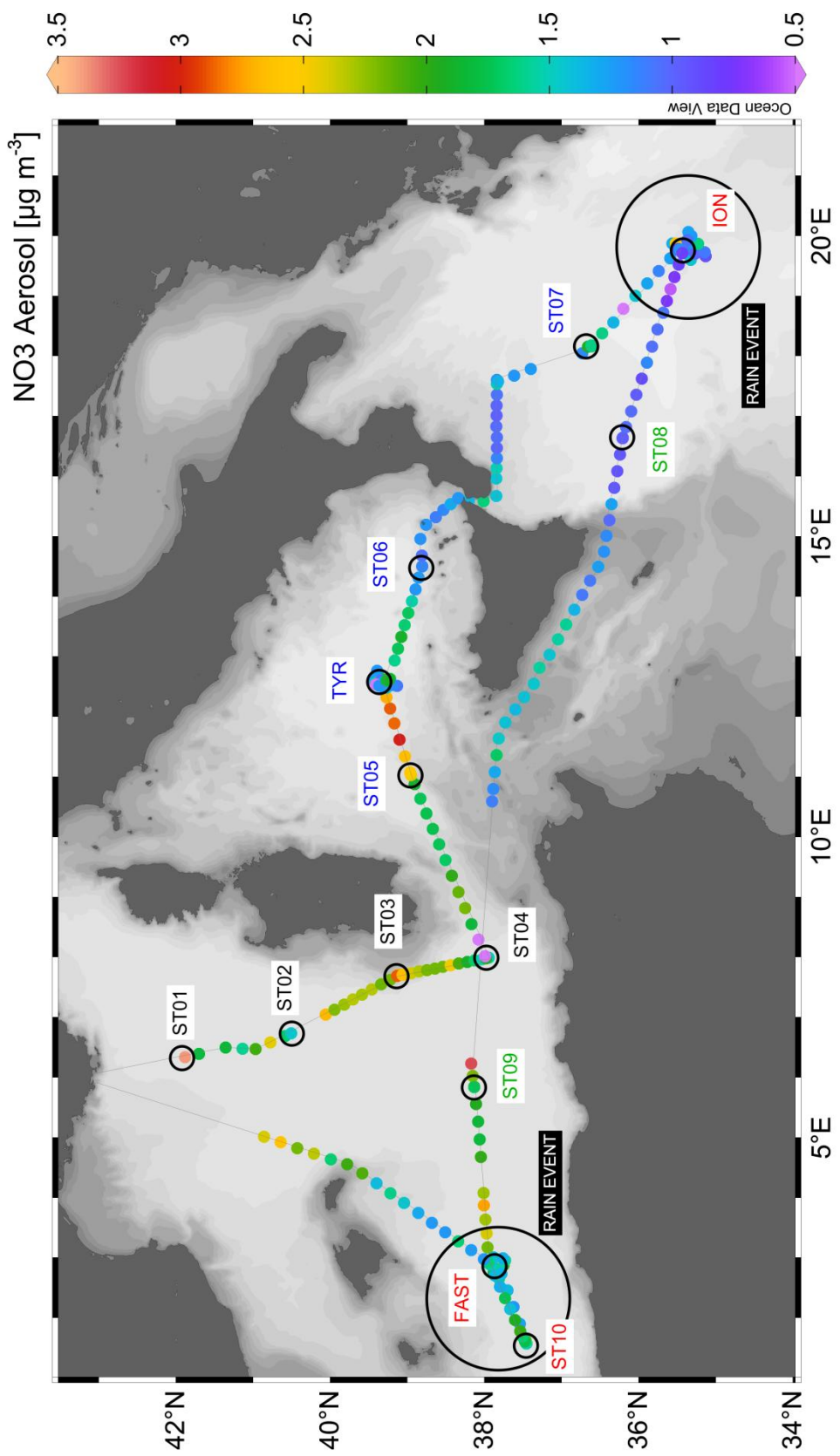
**Figure 5.** Evolution within the ML of heterotrophic prokaryotic production (BP), particulate 3190 primary production (PP), heterotrophic prokaryotes (hprok) and *Synechococcus* (syn) abundances at the FAST site. The mixed layer depth is indicated by a red line.

Supprimé: station  
Supprimé: in

**Figure 6.** Synthetic view of biogeochemical processes and exchanges between the ML and NDLb at the FAST site before the rain and evolution after the rain.

Supprimé: Figure 6. Results of the enrichment experiment. BP reached after 36 h of enrichment in the dark. C: control unamended, P:+DIP, N:+ $\text{NO}_3+\text{NH}_4$ , G:+glucose, and combinations of these elements in PN, NG, PG and NPG. Stars show significantly different BP compared to the unamended control . ¶  
Supprimé: 7

Fig. 1



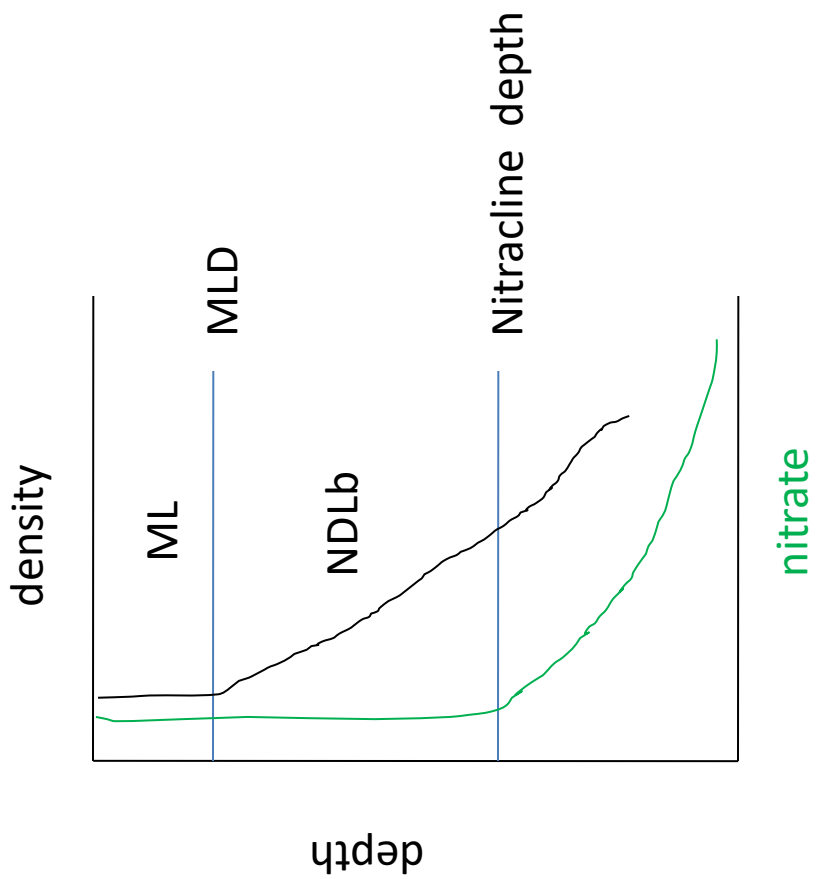


Fig.2

Fig. 3

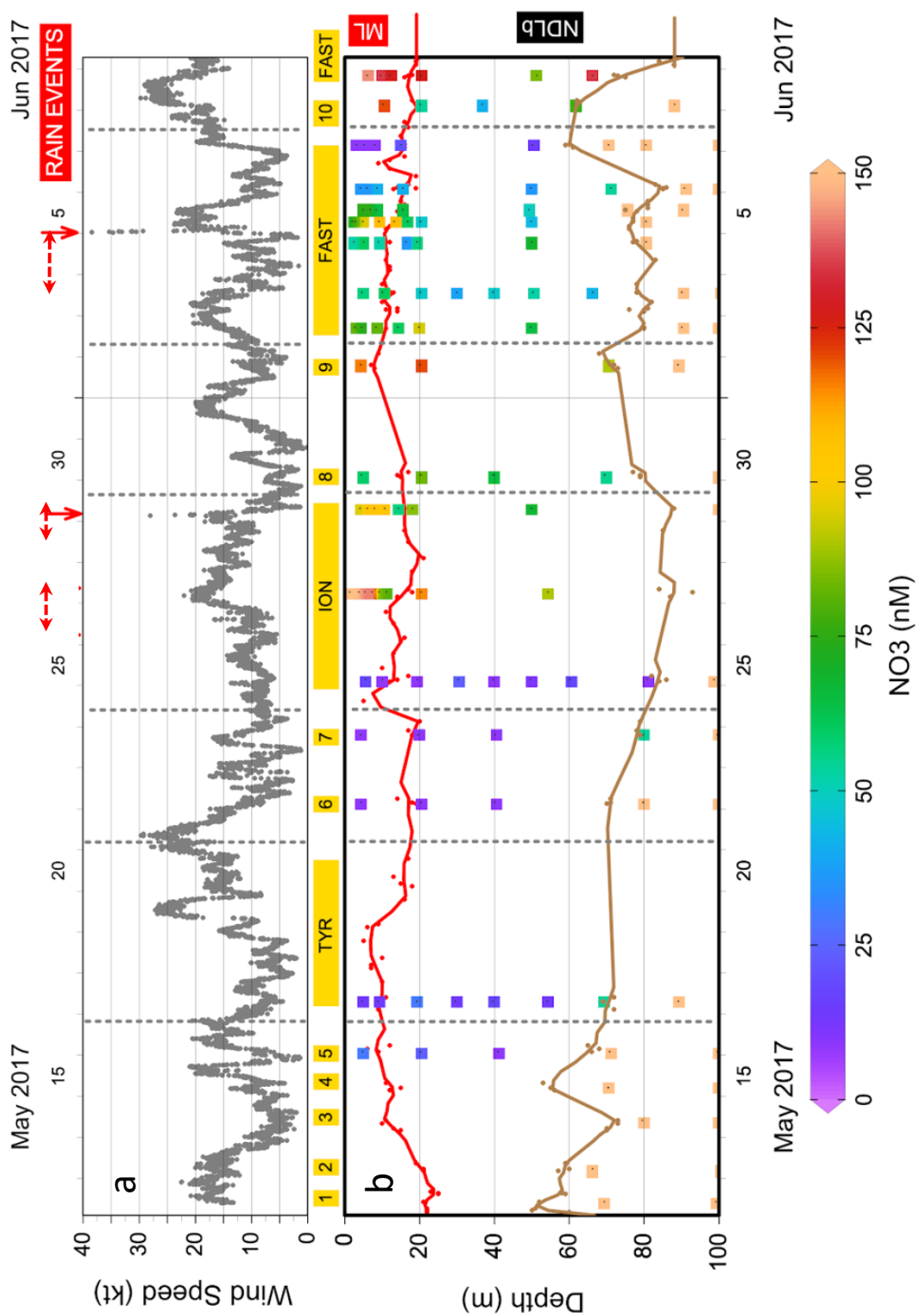


Fig. 4

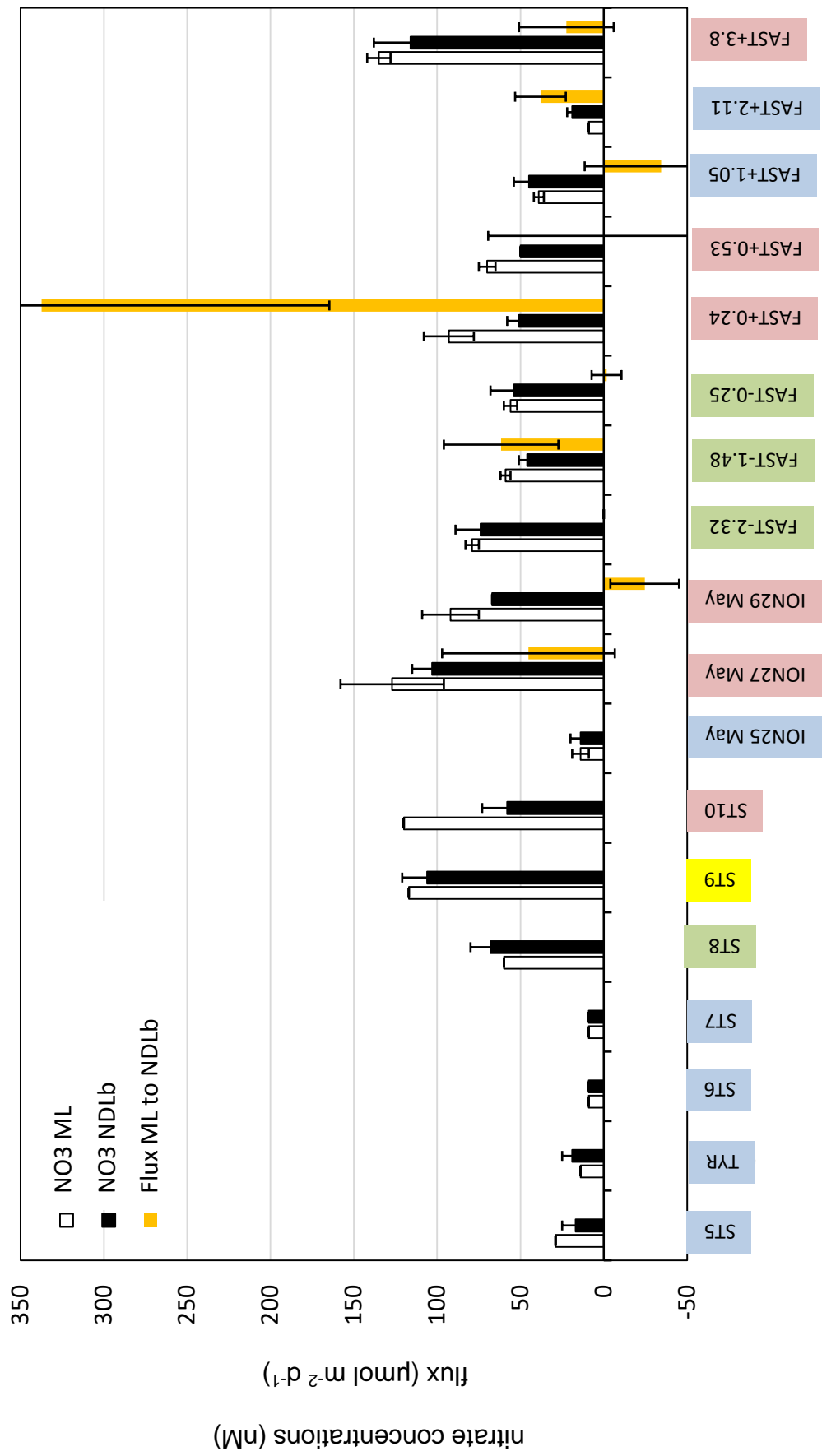


Fig. 5

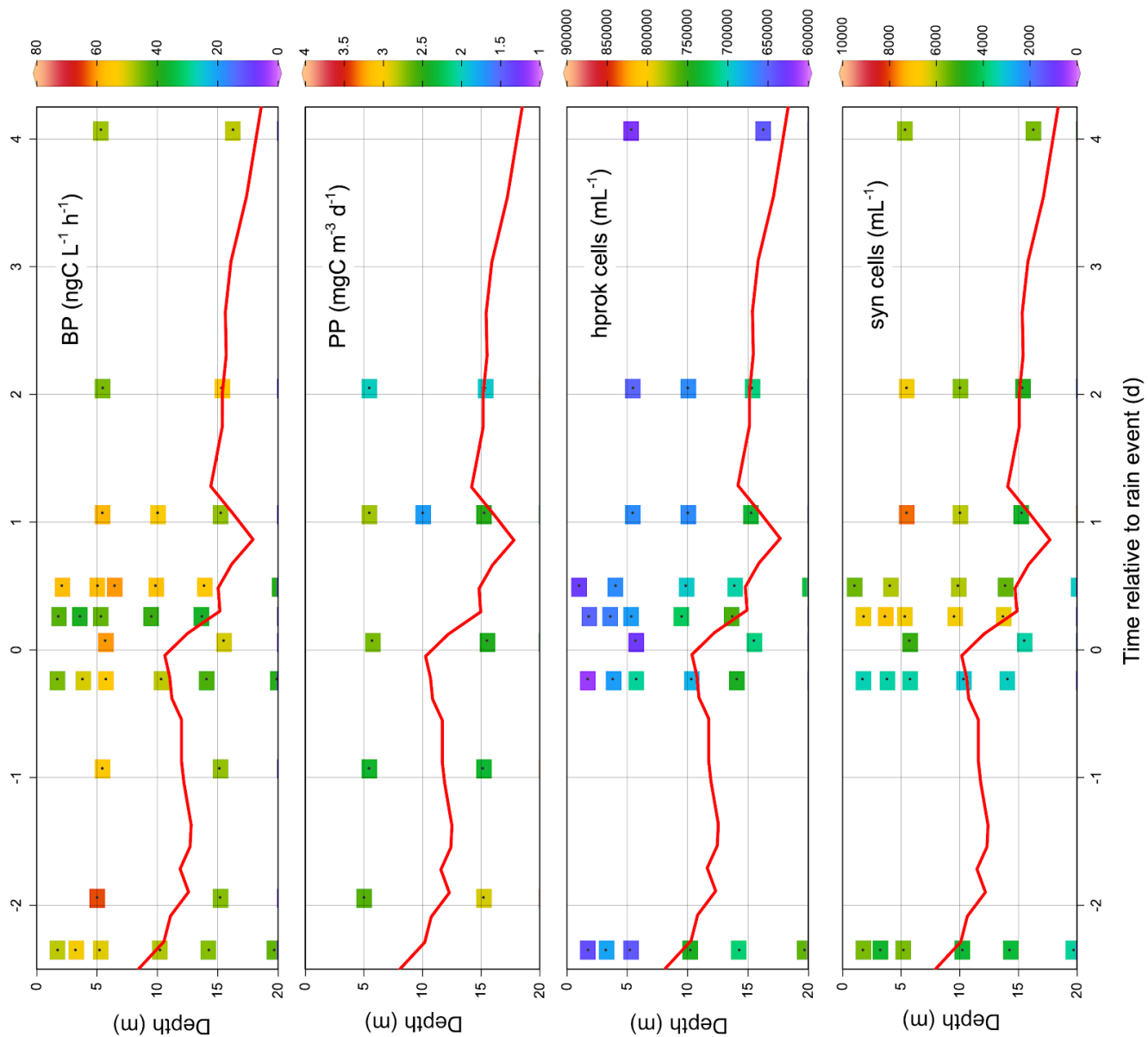
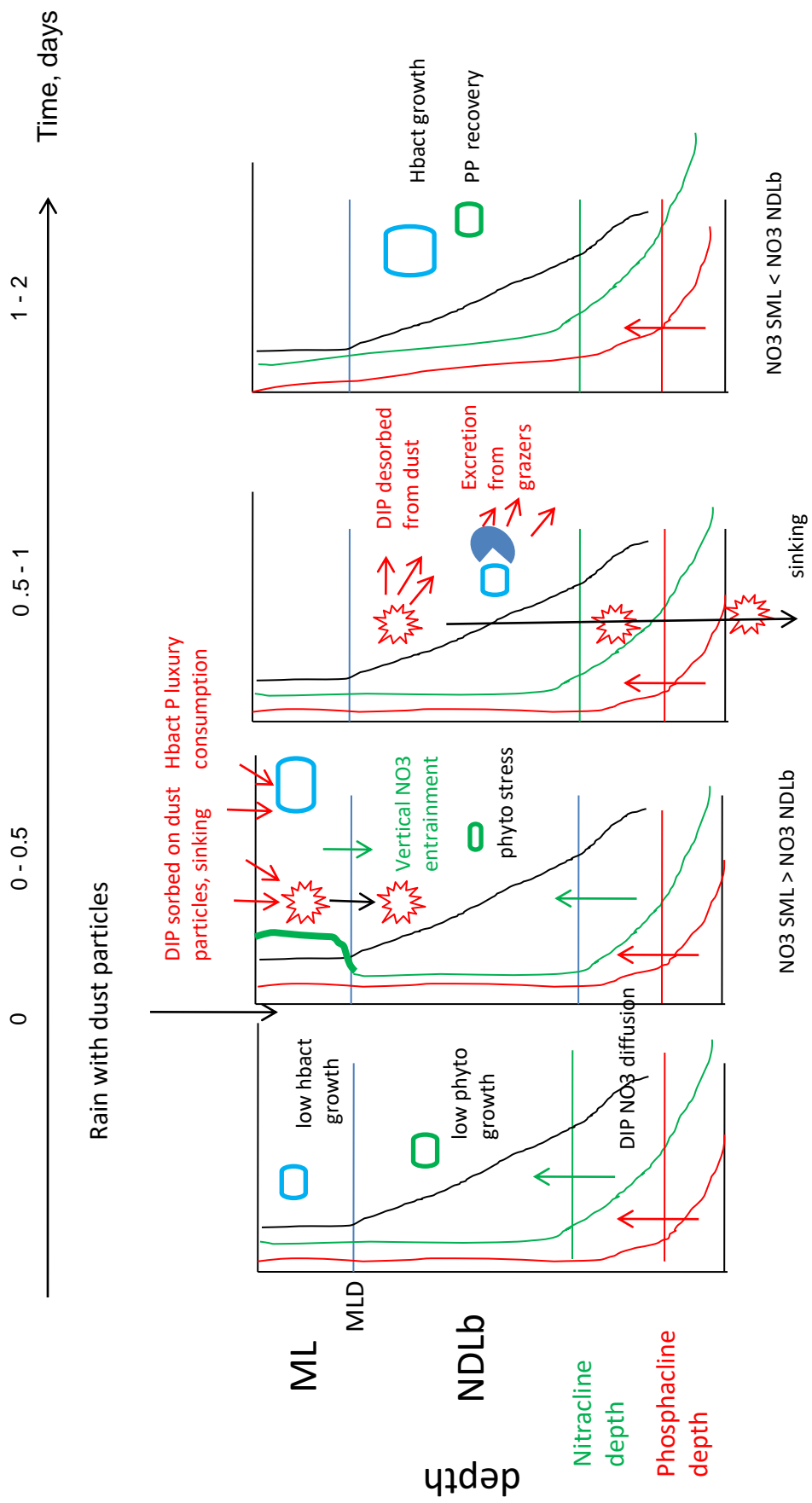


Fig. 6



## Supplementary information

[Page 1: Figure S1](#)

[Page 2: Figure S2](#)

[Page 3: Figure S3](#)

[Page 4: Enrichment experiment and Fig S4](#)

[Page 5: Table S1](#)

[Page 6: Table S2](#)

**Supprimé:** Influence of atmospheric deposition on biogeochemical cycles in an oligotrophic ocean system¶  
 France Van Wambeke<sup>1</sup>, Vincent Taillandier<sup>2</sup>, Karine Desboeufs<sup>3</sup>, Elvira Pulido-Villena<sup>1</sup>, Julie Dinasquet<sup>4,5</sup>, Anja Engel<sup>6</sup>, Emilio Marañón<sup>7</sup>, Céline Ridame<sup>8</sup>, Cécile Guieu<sup>2\*</sup>

**Mis en forme :** Distance de l'en-tête par rapport au bord : 1,2 cm, Distance du bas de page par rapport au bord : 0,8 cm

**Supprimé:** ¶  
 Figures legends¶

Figure S1: Vertical distribution of heterotrophic prokaryotic production (BP), particulate primary production (PP), and abundances of heterotrophic prokaryotes (hprok), *Synechococcus*-like cells (syn), eukaryotic picophytoplankton (pico euk) and nanophytoplankton (nano euk) at the ION site. Casts numbered the date of their sampling before (blue profiles) and after (grey profiles) the rain sampled onboard.

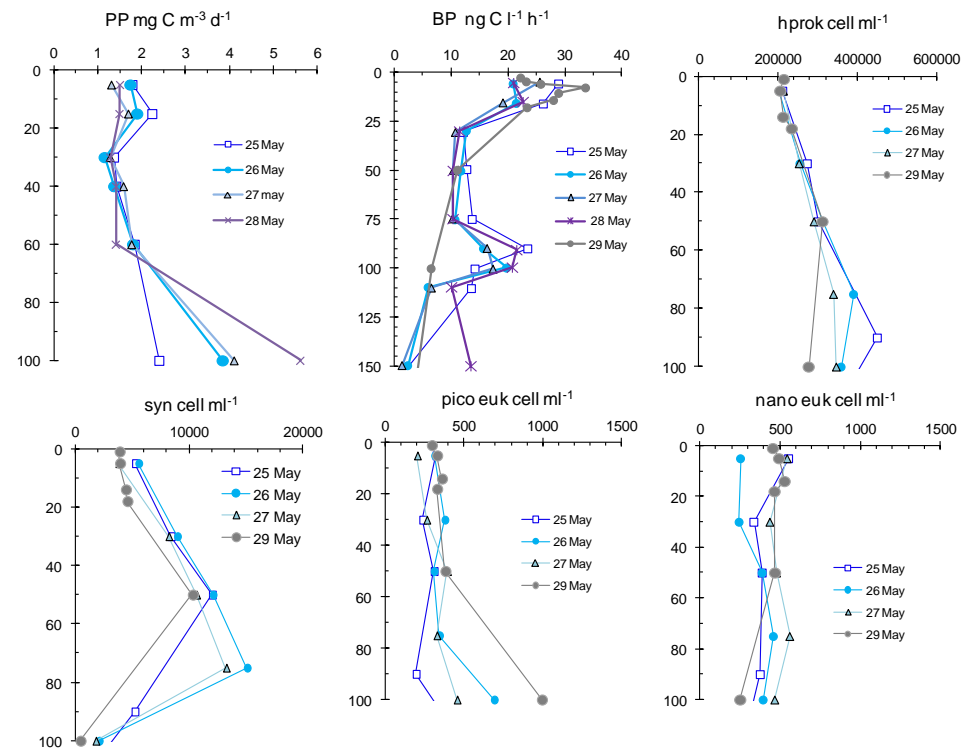


Figure S2: Vertical distribution of heterotrophic prokaryotic production (BP), particulate primary production (PP), and in vivo fluorescence profiles at [the](#) FAST site. Stations numbered in days before (blue profiles) and after (grey profiles) the rain event.

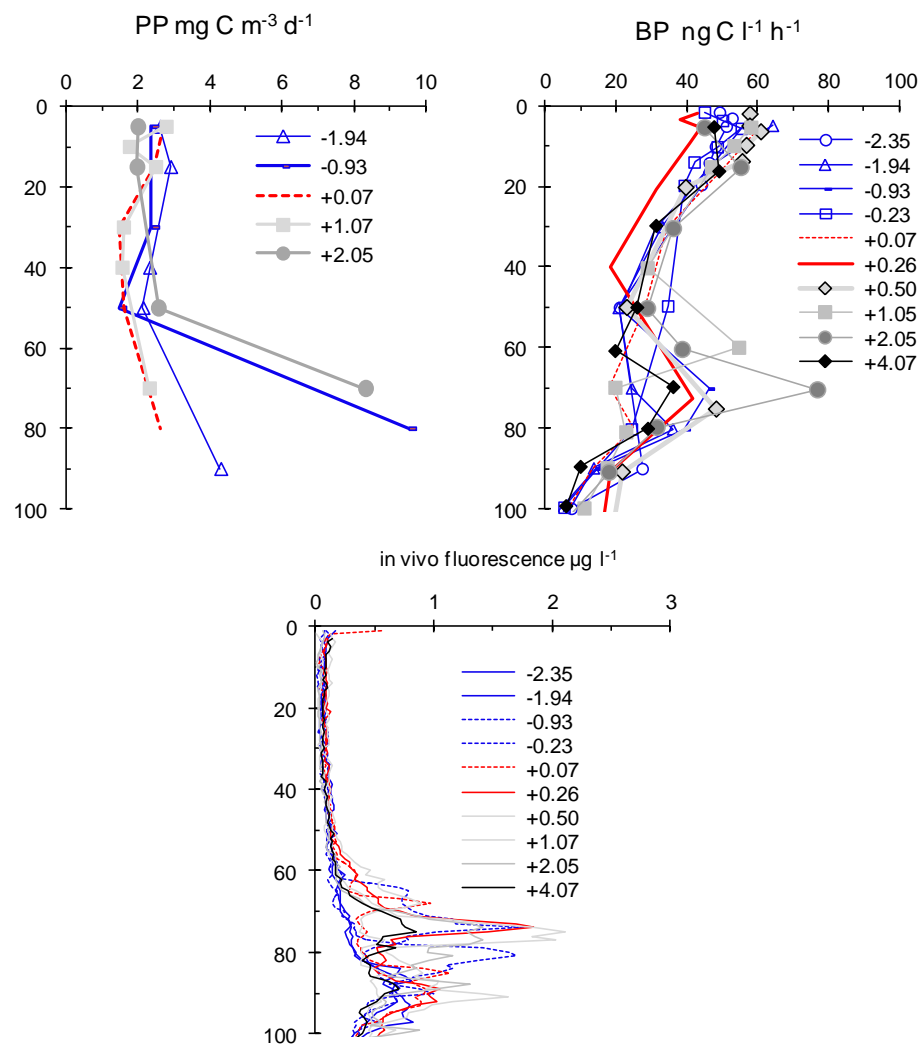
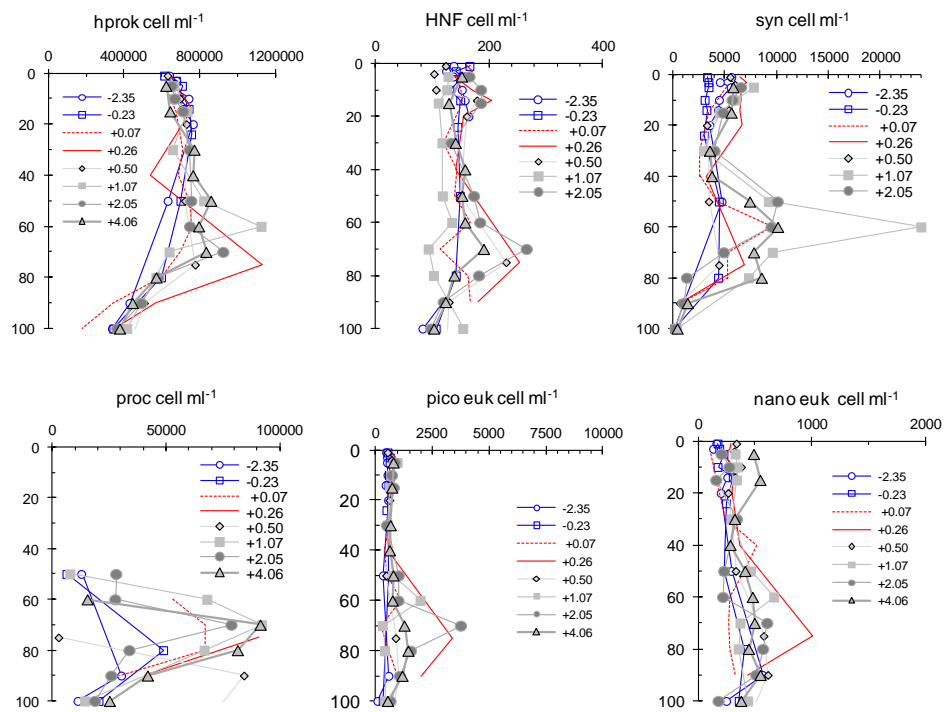


Figure S3. Vertical distribution of abundances for heterotrophic prokaryotes (hprok), heterotrophic nanoflagellates (HNF), *Synechococcus*-like cells (syn), *Prochlorococcus* (proc), eukaryotic picophytoplankton (pico euk) and nanophytoplankton (nano euk) at [the FAST site](#). Stations numbered in days before (blue profiles) and after (grey profiles) the rain event sampled on board.



### **Enrichment experiments**

At the three sites, enrichment experiments were performed using seawater from 5 m depth to assess factors limiting BP in the surface mixed layer. The sampling of seawater for these experiments [FAST (June 2, 22:00), TYR (May 16, 20:00) and ION (May 25, 20:00)] was done before the rain events occurring at the FAST and ION sites. Eight series of triplicate 60 mL polycarbonate bottles were filled with unfiltered seawater and amended as follows: C : no enrichment, N: +1  $\mu$ M NO<sub>3</sub> + 1  $\mu$ M NH<sub>4</sub>; P: + 0.2  $\mu$ M DIP; G: + 10  $\mu$ M C-glucose; NP: N + P; NG : N + G; PG : P + G; NPG: N + P + G. After 48 h incubation in the dark at *in situ* temperature, BP was determined in the 24 bottles (as described in M&M section).

At the TYR site, BP was significantly stimulated only after addition of 2 major elements, with a greater response with PN and NPG combinations (Fig. S4). At the ION site, BP was primarily limited by P availability, as only combinations with P (single or in combination with other elements), stimulated BP whereas all other combinations of enrichment did not stimulate BP significantly compared to the control. At the FAST site, BP was primarily limited by N availability, as all combinations with N, single or in combination with other elements, stimulated BP. However at this site it is likely that BP was also co-limited by 2 elements, as G addition alone also stimulated BP. Note that the PN combination has induced a higher stimulation of BP than other double combinations (NG or PG).

**Figure S4.** Results of the enrichment experiment. BP reached after 36 h of enrichment in the dark. C: control unamended, P: +DIP, N: +NO<sub>3</sub>+NH<sub>4</sub>, G: +glucose, and combinations of these elements in PN, NG, PG and NPG. Stars show significantly different BP compared to the unamended control.

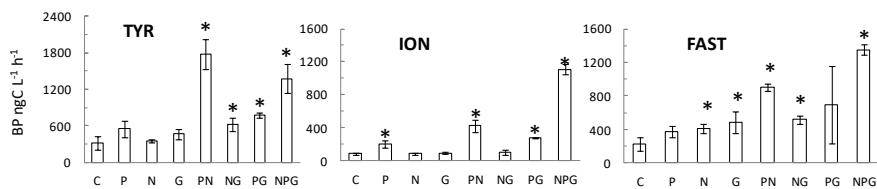


**Table S1:** NO<sub>3</sub> ranges within the surface mixed layer (ML) and the base of the nitrate depleted layer below (NDLb) and advective fluxes when measurable. FAST stations are chronologically indexed in days before (negative index) and after (positive index) the occurrence of the rain event. no lwcc: no data because at these stations concentrations were determined only by classical analysis and were under its detection limits (50 nM); na: not available. From comparison of concentrations, we identified four groups of stations: group 1: poor nitrates in ML and NDLb (< 50 nM); weak differences (< 15 nM); group 2: moderate nitrates in ML and NDLb (50 nM < NO<sub>3</sub> < 80 nM); weak differences (< 20 nM); group 3: high nitrate in ML and NDLb (NO<sub>3</sub> > 80 nM); weak positive differences (< 20 nM) and group 4: high nitrate in ML and moderate to high in NDLb, large positive differences (> 20 nM). MLD: mixed layer depth. sd of fluxes were estimated using propagation of errors on NO<sub>3</sub>ML, NO<sub>3</sub>NDLb and dMLD/dt.

|               | Date, local time | MLD<br>m | base NDLb<br>m | NO <sub>3</sub> in ML |          |    |                | NO <sub>3</sub> in NDLb |    |            |          | difference<br>nM | Flux SML to NDLb<br>μmol N m <sup>-2</sup> d <sup>-1</sup> | Station group |    |
|---------------|------------------|----------|----------------|-----------------------|----------|----|----------------|-------------------------|----|------------|----------|------------------|--|---------------|----|
|               |                  |          |                | Mean<br>nM            | sd<br>nM | n  | Mean nM        | sd nM                   | n  | Mean<br>nM | sd<br>nM | n                |  |               |    |
| ST 1          | 12/05/2017 12:26 | 21       | 52             | <u>no lwcc</u>        |          |    | <u>no lwcc</u> |                         |    | na         |          | na               | na   | na            | na |
| ST2           | 13/05/2017 07:40 | 21       | 60             | <u>no lwcc</u>        |          |    | <u>no lwcc</u> |                         |    | na         |          | na               | na   | na            | na |
| ST3           | 14/05/2017 12:05 | 11       | 73             | <u>no lwcc</u>        |          |    | <u>no lwcc</u> |                         |    | na         |          | na               | na   | na            | na |
| ST4           | 15/05/2017 07:09 | 15       | 55             | <u>no lwcc</u>        |          |    | <u>no lwcc</u> |                         |    | na         |          | na               | na   | na            | na |
| ST5           | 16/05/2017 04:04 | 9        | 66             | 29                    | 1        | 17 | 8              | 2                       | 13 | na         |          | 1                | 1  | 1             | 1  |
| ST TYR 17 May | 17/05/2017 09:36 | 9        | 69             | 14                    | 0        | 2  | 19             | 6                       | 4  | -5         | na       | 1                | 1  | 1             | 1  |
| ST6           | 22/05/2017 05:48 | 18       | 71             | 9                     | na       | 1  | 9              | 0                       | 2  | 0          | na       | 1                | 1  | 1             | 1  |
| ST7           | 23/05/2017 21:11 | 18       | 79             | 9                     | na       | 1  | 9              | 0                       | 2  | 0          | na       | 1                | 1  | 1             | 1  |
| STION 25 May  | 25/05/2017 05:28 | 14       | 86             | 14                    | 5        | 2  | 14             | 6                       | 6  | 0          | na       | 1                | 1  | 1             | 1  |
| STION 27 May  | 27/05/2017 08:24 | 18       | 93             | 127                   | 31       | 6  | 103            | 12                      | 2  | 24         | 45       | 52               | 4  | 4             | 4  |
| STION 29 May  | 29/05/2017 09:19 | 16       | 88             | 92                    | 17       | 6  | 67             | na                      | 1  | 25         | -25      | 21               | 4  | 4             | 4  |
| ST8           | 30/05/2017 04:48 | 14       | 79             | 60                    | na       | 1  | 68             | 12                      | 3  | -8         | na       | 2                | 2  | 2             | 2  |
| ST9           | 01/06/2017 21:15 | 7        | 72             | 117                   | na       | 1  | 106            | 15                      | 2  | 11         | na       | 3                | 3  | 3             | 3  |
| STFAST 2:3    | 02/06/2017 19:16 | 9        | 80             | 79                    | 4        | 3  | 74             | 15                      | 3  | 6          | 0        | 0                | 2  | 2             | 2  |
| ST FAST -1:5  | 03/06/2017 15:30 | 13       | 78             | 59                    | 3        | 2  | 46             | 5                       | 5  | 13         | 62       | 34               | 2  | 2             | 2  |
| ST FAST -0:25 | 04/06/2017 20:57 | 12       | 77             | 56                    | 4        | 3  | 54             | 14                      | 3  | 2          | -2       | 9                | 2  | 2             | 2  |
| ST FAST +0:24 | 05/06/2017 08:54 | 16       | 77             | 93                    | 15       | 5  | 51             | 7                       | 3  | 42         | 337      | 173              | 4  | 4             | 4  |
| ST FAST +0:53 | 05/06/2017 15:50 | 16       | 82             | 70                    | 5        | 4  | 50             | na                      | 1  | 20         | 0        | 69               | 4  | 4             | 4  |
| ST FAST +1:05 | 06/06/2017 04:23 | 19       | 85             | 39                    | 3        | 4  | 45             | 9                       | 2  | -6         | -34      | 46               | 1  | 1             | 1  |
| ST FAST +2:11 | 07/06/2017 05:38 | 15       | 59             | 9                     | 0        | 3  | 19             | 3                       | 2  | -10        | 38       | 15               | 1  | 1             | 1  |
| ST10          | 08/06/2017 06:55 | 19       | 62             | 120                   | na       | 1  | 58             | 15                      | 3  | 62         | na       | 4                | 4  | 4             | 4  |
| ST FAST +3:8  | 08/06/2017 22:09 | 17       | 73             | 135                   | 7        | 3  | 116            | 22                      | 3  | 20         | 22       | 28               | 4  | 4             | 4  |

**Mis en forme :** Retrait : Première ligne : 0,75 cm  
**Mis en forme :** Haut : 0,9 cm, Bas : 0,9 cm, Distance du bas de page par rapport au bord : 0,2 cm  
**Supprimé:** na: not available because under LWCC detection limits  
**Supprimé:** ¶

**Table S2.** Biological stocks and fluxes integrated over the mixed layer (a), the euphotic zone (b) and 200 m (c), along with atmospheric dry deposition during the occupation of the ION and FAST sites. Time\_CTD east is the local time at the beginning of the CTD cast. For atmospheric dry deposition, start and end shows the period during which PLIS data were averaged to compute daily NO<sub>3</sub> depositions fluxes. PP: Primary production, BP: heterotrophic prokaryotic production, LAP: *In situ* leucine aminopeptidase hydrolysis rates, N<sub>2</sub>fix : N<sub>2</sub> fixations rates.

| -          | time_CTD<br>east | biological flux   |   |  |  |  |   | stocks  |       |               | dry deposition   |      |  |
|------------|------------------|---|---|--|--|--|---|---|-------|---------------|--|------|--|
|            |                  | PP <sup>b</sup><br>mg C m <sup>-2</sup> d <sup>-1</sup> | BP <sup>c</sup><br>mg C m <sup>-2</sup> d <sup>-1</sup> | PP_ML <sup>a</sup><br>mg C m <sup>-2</sup> d <sup>-1</sup> | BP_ML <sup>a</sup><br>mg C m <sup>-2</sup> d <sup>-1</sup> | N <sub>2</sub> fix_ML <sup>a</sup><br>μmol N m <sup>-2</sup> d <sup>-1</sup> | NO <sub>3</sub> stocks<br>ML <sup>a</sup><br>μmol N m <sup>-2</sup> | DIP stocks<br>ML <sup>a</sup><br>μmol P m <sup>-2</sup> | start | end           | NO <sub>3</sub><br>μmole N m <sup>-2</sup> d <sup>-1</sup> |      |  |
| TYR 17 May | 17/5/17 4:58     |   |   | 5.6  | 13.7   | 5.6  | 3.9   | 127   | 64    | 17/5/17 2:54  | 17/5/17 4:58   | 23.2 |  |
| TYR 18 May | 18/5/17 4:57     |   |   | 6.0  | 12.0   | 6.0  |   |   |       | 17/5/17 4:58  | 18/5/17 4:57   | 25.1 |  |
| TYR 19 May | 19/5/17 4:53     |   |   | 6.1  | 13.9   | 6.1  |   |   |       | 18/5/17 4:57  | 19/5/17 4:53   | 26.9 |  |
| TYR 20 May | 20/5/17 4:45     |   |   | 14.5   | 46.1   | 14.5   |   |   |       | 19/5/17 4:53  | 20/5/17 4:45   | 37.9 |  |
| ION 25 May | 25/5/17 4:34     | 188   | 56.1  | 19.7   | 7.5  | 27.8   | 6.1   | 195   | 142   | 24/5/17 18:02 | 25/5/17 4:34   | 24.1 |  |
| ION 26 May | 26/5/17 4:25     | 207   | 44.7  | 26.9   | 8.0  | -  | -   | -   | -     | 25/5/17 4:34  | 26/5/17 4:25   | 27.8 |  |
| ION 27 May | 27/5/17 4:26     | 210   | 43.9  | 19.9   | 8.0  | -  | 5.1   | 2113  | 109   | 26/5/17 4:25  | 27/5/17 4:26   | 32.6 |  |
| ION 28 May | 28/5/17 4:21     | 226   | -   | 31.3   | 10.7   | -  | -   | -   | -     | 27/5/17 4:26  | 28/5/17 4:21   | 33.8 |  |
| ION 29 May | 29/5/17 9:19     | -   | 45.2  | -  | 10.3   | -  | 6.3   | 1477  | 167   | 28/5/17 4:21  | 29/5/17 9:19   | 29.2 |  |
| FAST 2.32  | 2/6/17 18:37     | -   | -   | -  | -  | -  | -   | -   | -     | -             | -  | -    |  |
| FAST-1.48  | 3/6/17 4:32      | 257   | 81.2  | 37.8   | 9.9  | 31.1   | -   | 715   | 29    | 2/6/17 20:24  | 2/6/17 18:37   | -    |  |
| FAST-0.93  | 4/6/17 4:40      | 274   | 87.9  | 28.5   | 5.6  | -  | 5.9   | 751   | 162   | 2/6/17 18:37  | 3/6/17 4:32  | 42.5 |  |
| FAST-0.25  | 4/6/17 21:27     | -   | 88.9  | -  | 1.24   | -  | 7.1   | -   | -     | 3/6/17 4:32   | 4/6/17 4:40  | 38.3 |  |
| FAST 0.07  | 5/6/17 4:44      | 164   | 80.8  | 29.3   | 15.6   | -  | 6.4   | 665   | 137   | 4/6/17 4:40   | 4/6/17 21:27   | 61.2 |  |
| FAST 0.24  | 5/6/17 9:24      | -   | 92.7  | -  | 14.6   | 47.2   | -   | 1520  | 136   | 4/6/17 21:27  | 5/6/17 4:44  | 39.6 |  |
| FAST 0.53  | 5/6/17 14:59     | -   | 113.3   | -  | 19.4   | 52.8   | -   | 1113  | 210   | 5/6/17 4:44   | 5/6/17 9:24  | -    |  |
| FAST 1.05  | 6/6/17 4:51      | 140   | 99.2  | 33.4   | 8.6  | 54.8   | 8.3   | 752   | 281   | 5/6/17 14:59  | 6/6/17 4:51  | -    |  |
| FAST 2.11  | 7/6/17 4:17      | 218   | 104.1   | 31.8   | 18.7   | 35.1   | 8.1   | 177   | 194   | 6/6/17 4:51   | 7/6/17 4:17  | 19.8 |  |
| FAST 3.8   | 9/6/17 4:40      | -   | 82.9  | -  | 21.9   | 34.5   | -   | 2314  | 125   | 8/6/17 21:06  | 9/6/17 0:16  | 23.9 |  |